



CIVIL ENGINEERING STUDIES  
Illinois Center for Transportation Series No. 09-032  
UIIU-ENG-2009-2002  
ISSN: 0197-9191

# PERFORMANCE OF I-57 RECYCLED CONCRETE PAVEMENTS

Prepared By

**Jeffrey R. Roesler**  
**J. Gregory Huntley**

University of Illinois at Urbana-Champaign

Research Report ICT-09-032

A report of the findings of

**ICT-R41**

**Performance of I-57 Recycled Concrete Pavements**

Illinois Center for Transportation

January 2009

## Technical Report Documentation Page

<b>1. Report No.</b> FHWA-ICT-09-032	<b>2. Government Accession No.</b>	<b>3. Recipient's Catalog No.</b>	
<b>4. Title and Subtitle</b>  PERFORMANCE OF I-57 RECYCLED CONCRETE PAVEMENT		<b>5. Report Date</b> January 9, 2009	
		<b>6. Performing Organization Code</b>	
<b>7. Author(s)</b> Jeffrey Roesler and J. Gregory Huntley		<b>8. Performing Organization Report No.</b> ICT-09-032 UILU-ENG-2009-2002	
<b>9. Performing Organization Name and Address</b>  University of Illinois at Urbana-Champaign Department of Civil and Environmental Engineering 205 North Matthews Ave. Urbana, IL 61801		<b>10. Work Unit (TRAVIS)</b>	
		<b>11. Contract or Grant No.</b> R 27-41	
		<b>13. Type of Report and Period Covered</b> Final Report Jan 2008 to December 2008	
<b>12. Sponsoring Agency Name and Address</b> Illinois Department of Transportation Bureau of Material and Physical Research 126 East Ash Street Springfield, IL 62704		<b>14. Sponsoring Agency Code</b>	
<b>15. Supplementary Notes</b>			
<b>16. Abstract</b>  In 1986-1987 the Illinois Department of Transportation (IDOT) constructed a demonstration project on I-57 near Effingham, Illinois to evaluate the viability of recycling an existing jointed reinforced concrete pavement for use as its primary aggregates in the surface mixture of a 10-in continuously reinforced concrete pavement (CRCP). This CRCP test section on northbound and southbound I-57 contained a 7-in cement-stabilized subbase and a 13.5-ft extended lane width. Longitudinal reinforcement bars were placed using the tube feeding method. Functional and structural data, including falling weight deflectometer testing (FWD), distress surveys, friction testing, surface profile testing, and conditions rating surveys were collected periodically throughout the life of the pavement. Structural test data demonstrates a pavement section that has exhibited excellent load carrying capacity (less than 0.006-in deflection under 9-kip load), and load transfer efficiency across the transverse cracks. Furthermore, the cement-treated subbase and subgrade have performed well over the CRCP's service life. There also was no structural response or cracking difference between the sections with the stabilized base extended under the shoulder versus the base that is only a standard lane width.  Few structural distresses are observed except for the prominent amount of longitudinal cracking that appears over the reinforcement bars in all lanes. This abnormal cracking pattern has been noted for many years and has been attributed to settlement cracking associated with the original tube feeding process, the bar size selected, the bulk density of the concrete with recycled concrete aggregate (RCA), and the higher drying shrinkage of RCA concrete. The section has developed a significant amount of localized distresses and patches over the past 5 years as a result of the further deterioration of this longitudinal cracking distress. A petrographic examination has concluded that there is no deleterious alkali-silica reaction occurring in the RCA test section, and that the air void system is normal. The mean transverse crack spacing is approximately 1.5 ft, which is significantly shorter than normal CRCP and can be attributed to the greater drying shrinkage potential, slightly lower tensile strength, and reduced fracture properties of RCA. Functionally, the pavement shows good skid resistance and fair-to-good ride quality. Overall, the performance of this CRCP pavement with RCA has exceeded roughly 50 percent of the 10-in CRCP within Illinois in terms of age and 25 percent in terms of traffic.  Based on the 20 years of performance on the I-57 CRCP section, the future use of RCA on concrete pavement in Illinois can be approached with confidence and optimism. IDOT's original material assessment has avoided any material-related distress such as freeze-thaw damage (D-cracking), ASR, and corrosion of the steel from excess chloride content. Future application of RCA in concrete pavements should consider its higher drying shrinkage potential and lower tensile strength and fracture energy. Future implementation of moist curing on concrete pavements with RCA or use of two-lift construction technique would minimize risk of the extremely close crack spacing due to excessive drying shrinkage noted on the I-57 CRCP test section.			
<b>17. Key Words</b> Recycled Concrete Aggregate, continuously reinforced concrete pavement, performance		<b>18. Distribution Statement</b> No restrictions. This document is available to the public through the National Technical Information Service, Springfield, Virginia 22161.	
<b>19. Security Classif. (of this report)</b> Unclassified	<b>20. Security Classif. (of this page)</b> Unclassified	<b>21. No. of Pages</b> 88	<b>22. Price</b>

## **ACKNOWLEDGEMENT, DISCLAIMER, MANUFACTURERS' NAMES**

This publication is based on the results of ICT-R27-41, *Performance of I-57 Recycled Concrete Pavement*. ICT-R27-41 was conducted in cooperation with the Illinois Center for Transportation; the Illinois Department of Transportation; and the U.S. Department of Transportation, Federal Highway Administration.

Members of the Technical Review Panel are the following:

Mark Gawedzinski, Illinois Department of Transportation (chair)

Sheila Beshears, Illinois Department of Transportation

Doug Dirks, Illinois Department of Transportation

Terry Hoekstra, Illinois Department of Transportation

Brian Pfeifer, Federal Highway Administration

Amy Schutzbach, Illinois Department of Transportation

Dan Tobias, Illinois Department of Transportation

The authors would also like to acknowledge the contribution of Dr. Karl Peterson of Michigan Technological University for his petrographic examination of the concrete cores that were extracted from the I-57 CRCP experimental section. His work was extremely valuable in assessing whether there was any materials-related distress such as deleterious ASR cracking. Dr. Peterson's summary report is included in Appendix A. The authors would also like to thank Dr. Mark Snyder for his assistance in locating old reports and data from his early national study on recycled concrete pavement and Ms. Maria Quinones for her assistance in analyzing the CRCP video distress data.

The contents of this report reflect the view of the authors, who are responsible for the facts and accuracy of the data presented herein. The contents do not necessarily reflect the official views or policies of the Illinois Center for Transportation, the Illinois Department of Transportation, or the Federal Highway Administration. This report does not constitute a standard, specification, or regulation.

Trademark or manufacturers' names appear in this report only because they are considered essential to the object of this document and do not constitute an endorsement of product by the Federal Highway Administration, the Illinois Department of Transportation, or the Illinois Center for Transportation.

## EXECUTIVE SUMMARY

In 1986-1987 the Illinois Department of Transportation (IDOT) constructed a demonstration project on I-57 near Effingham, Illinois to evaluate the viability of recycling an existing jointed reinforced concrete pavement for use as its primary aggregates in the surface mixture of a 10-in continuously reinforced concrete pavement (CRCP). This CRCP test section on northbound and southbound I-57 contained a 7-in cement-stabilized subbase and a 13.5-ft extended lane width. Longitudinal reinforcement bars were placed using the tube feeding method. Functional and structural data, including falling weight deflectometer testing (FWD), distress surveys, friction testing, surface profile testing, and conditions rating surveys were collected periodically throughout the life of the pavement. Structural test data demonstrates a pavement section that has exhibited excellent load carrying capacity (less than 0.006-in deflection under 9-kip load), and load transfer efficiency across the transverse cracks. Furthermore, the cement-treated subbase and subgrade have performed well over the CRCP's service life. There also was no structural response or cracking difference between the sections with the stabilized base extended under the shoulder versus the base that is only a standard lane width.

Few structural distresses are observed except for the prominent amount of longitudinal cracking that appears over the reinforcement bars in all lanes. This abnormal cracking pattern has been noted for many years and has been attributed to settlement cracking associated with the original tube feeding process, the bar size selected, the bulk density of the concrete with recycled concrete aggregate (RCA), and the higher drying shrinkage of RCA concrete. The section has developed a significant amount of localized distresses and patches over the past 5 years as a result of the further deterioration of this longitudinal cracking distress. A petrographic examination has concluded that there is no deleterious alkali-silica reaction occurring in the RCA test section, and that the air void system is normal. The mean transverse crack spacing is approximately 1.5 ft, which is significantly shorter than normal CRCP and can be attributed to the greater drying shrinkage potential, slightly lower tensile strength, and reduced fracture properties of RCA. Functionally, the pavement shows good skid resistance and fair-to-good ride quality. Overall, the performance of this CRCP pavement with RCA has exceeded roughly 50 percent of the 10-in CRCP within Illinois in terms of age and 25 percent in terms of traffic.

Based on the 20 years of performance on the I-57 CRCP section, the future use of RCA on concrete pavement in Illinois can be approached with confidence and optimism. IDOT's original material assessment has avoided any material-related distress such as freeze-thaw damage (D-cracking), ASR, and corrosion of the steel from excess chloride content. Future application of RCA in concrete pavements should consider its higher drying shrinkage potential and lower tensile strength and fracture energy. Future implementation of moist curing on concrete pavements with RCA or use of two-lift construction technique would minimize risk of the extremely close crack spacing due to excessive drying shrinkage noted on the I-57 CRCP test section.

# CONTENTS

<b>ACKNOWLEDGEMENT, DISCLAIMER, MANUFACTURERS' NAMES</b> .....	<b>i</b>
<b>EXECUTIVE SUMMARY</b> .....	<b>ii</b>
<b>CHAPTER 1. INTRODUCTION</b> .....	<b>1</b>
1.1 OVERVIEW.....	1
1.2 RESEARCH OBJECTIVE .....	1
1.3 PROJECT TASKS.....	1
<b>CHAPTER 2. LITERATURE REVIEW</b> .....	<b>3</b>
2.1 PURPOSE OF LITERATURE REVIEW .....	3
2.2 RCA FRESH CONCRETE PROPERTIES .....	3
2.2.1 Workability.....	3
2.2.2 Air Content .....	4
2.3 HARDENED CONCRETE PROPERTIES.....	4
2.3.1 Strength.....	4
2.3.2 Modulus of Elasticity.....	5
2.3.3 Creep .....	5
2.3.4 Drying Shrinkage.....	5
2.3.5 Coefficient of Thermal Expansion .....	5
2.3.6 Durability .....	5
2.3.7 Aggregate Freeze–Thaw Durability.....	6
2.3.8 Alkali-Silica Reactive Aggregates .....	6
2.4 Performance Summary of RCA in Concrete Pavements .....	7
<b>CHAPTER 3. I-57 RECYCLED CRCP PROJECT SUMMARY</b> .....	<b>8</b>
3.1 OVERVIEW.....	8
3.2 GENERAL INFORMATION.....	8
3.3 PREVIOUS JRC PAVEMENT SECTION.....	9
3.4 STRUCTURAL DESIGN OF CRCP INLAY.....	9
3.5 PAVEMENT MATERIALS .....	10
3.6 CONCRETE MIXTURE DESIGN .....	11
3.7 CONSTRUCTION METHODS .....	12
3.7.1 Subbase Stabilization.....	13
3.7.2 Steel Reinforcement Placement.....	13
3.8 FRESH CONCRETE PROPERTIES.....	13
3.9 TRAFFIC LOADINGS .....	13
<b>CHAPTER 4. PREVIOUS I-57 CRCP RESEARCH</b> .....	<b>16</b>
4.1 RECYCLED MATERIALS RESOURCE CENTER SURVEY .....	16
4.2 ILLINOIS LONGITUDINAL CRACKING INVESTIGATION .....	19
4.2.1 Field Survey and Coring (2002) .....	19
4.2.2 Laboratory Investigation of CRC Field Slabs (2003).....	19
4.2.3 Petrographic Examination of CRCP Field Cores (Peterson, 2008).....	20
<b>CHAPTER 5. STRUCTURAL EVALUATION</b> .....	<b>22</b>
5.1 FALLING WEIGHT DEFLECTION (FWD) DATA.....	22
5.1.1 Deflection and Deflection AREA.....	23
5.2.2 Load Transfer Efficiency (LTE).....	28
5.2.3 Subgrade Resilient Modulus .....	31
5.2.4 Modulus of Subgrade Reaction .....	32
5.2.5 Elastic Modulus ( $E_c$ ).....	32

5.3 DISTRESS SURVEYS .....	33
5.3.1 Longitudinal Cracking.....	33
5.3.2 Localized Distresses, Patches, and Punchouts .....	34
5.3.3 Mean Crack Spacing .....	38
5.4 PAVEMENT STRUCTURAL PERFORMANCE .....	41
<b>CHAPTER 6. FUNCTIONAL EVALUATION .....</b>	<b>41</b>
6.1 FRICTION TESTING.....	41
6.2 INTERNATIONAL ROUGHNESS INDEX .....	43
6.3 CONDITION RATING SURVEY (CRS).....	44
6.4 SUMMARY OF I-57 FUNCTIONAL PERFORMANCE.....	45
<b>CHAPTER 7. PERFORMANCE OF COMPARABLE CRCP IN ILLINOIS.....</b>	<b>45</b>
<b>CHAPTER 8. RECOMMENDATIONS FOR FUTURE RECYCLED CONCRETE</b>	
<b>PAVEMENTS IN ILLINOIS .....</b>	<b>46</b>
<b>CHAPTER 9. CONCLUSIONS .....</b>	<b>46</b>
<b>CHAPTER 10. REFERENCES .....</b>	<b>48</b>
<b>APPENDIX A. Report on Petrographic Examination of Cores from Concrete</b>	
<b>Pavement .....</b>	<b>A.1</b>

## LIST OF FIGURES

Figure 1. Original pavement cross section (Schutzbach, 1993).....	9
Figure 2. Cross section of I-57 CRC pavement inlay with RCA (Schutzbach, 1993).....	10
Figure 3. I-57 fractured core under ultra-violet light and coated with uranyl acetate dihydrate (Sturtevant, 1997).....	17
Figure 4. Expansion versus time for modified mortar bar expansion – ASTM C1293 (Sturtevant, 2007) .....	18
Figure 5. Photo of void filled with ASR gel from Illinois CRCP test section (Sturtevant, 2007).....	18
Figure 6. Average center of the driving lane deflection per direction per year .....	24
Figure 7. Average center of the driving lane AREA per direction per year .....	25
Figure 8. Average northbound center of the driving lane AREA per year .....	26
Figure 9. Average northbound center of the driving lane deflection per year .....	26
Figure 10. Average southbound center of the driving lane AREA per year .....	27
Figure 11. Average southbound center of the driving lane deflection per year .....	27
Figure 12. Load transfer efficiency at leave crack of outer wheel path .....	30
Figure 13. Longitudinal cracking in the northbound lane .....	34
Figure 14. Longitudinal cracking and distress in the northbound driving lane .....	34
Figure 15. Localized distress in the southbound driving lane .....	36
Figure 16. Deteriorating patch in the southbound driving lane.....	37
Figure 17. Multiple CRCP patches in the southbound driving lane.....	37
Figure 18. Transverse cracking northbound lanes.....	40
Figure 19. Transverse and longitudinal cracking northbound lanes.....	40
Figure 20. Changes in treaded and smooth friction data over time .....	43
Figure 21. I-57 average IRI per year per direction .....	43
Figure 22. CRS values of pavement life.....	45

## LIST OF TABLES

Table 1. Summary of RCA Concrete Pavement Site Locations (Sturtevant, 2007) .....	7
Table 2. Summary of RCA Concrete Pavement Features (Sturtevant, 2007) .....	8
Table 3. I-57 Recycled Concrete Aggregate Gradations (Schutzbach, 1993) .....	11
Table 4. Recycled Concrete Aggregate Quality Tests (Schutzbach, 1993) .....	11
Table 5. 1986 Concrete Mixture Design (Schutzbach, 1993) .....	12
Table 6. 1987 Mix Design Quantities (Schutzbach, 1993) .....	12
Table 7. I-57 Traffic History and Estimated ESALs in Design Lane .....	14
Table 8. I-57 Field and Laboratory Performance Data and Average RCA and Control Pavement Performance Data (after Sturtevant, 2007) .....	16
Table 9. Location and Nomenclature for Extracted CRCP Cores .....	21
Table 10. FWD Testing Dates and Locations .....	22
Table 11. Northbound Center Panel Averages for Deflection and AREA .....	23
Table 12. Southbound Center Panel Averages for Deflection and AREA .....	24
Table 13. Average Northbound True Edge Deflection and AREA .....	28
Table 14. Average Southbound True Edge Deflection and AREA .....	28
Table 15. Average Northbound LTE – Outer Wheel Path .....	29
Table 16. Average Southbound LTE – Outer Wheel Path .....	29
Table 17. Average Northbound LTE – Striped Edge .....	30
Table 18. Average Southbound LTE – Striped Edge .....	30
Table 19. Average Northbound $E_{RI}$ , $k$ -value and $E_C$ per Year .....	31
Table 20. Average Southbound $E_{RI}$ , $k$ -value and $E_C$ per Year .....	31
Table 21. Total Number of Popouts, Potholes, and Punchouts Identified on Visual Distress Surveys .....	35
Table 22. Total Number of Patches, Punchouts and Localized Distresses Identified on Video Distress Surveys .....	36
Table 23. 2002 Mean Crack Spacing and Location on I-57 (Location 1) .....	38
Table 24. 2002 Mean Crack Spacing and Location on I-57 (Location 2) .....	39
Table 25. 2007 Mean Crack Spacing and Location on I-57 .....	39
Table 26. Observed Crack Spacing and Location on I-39 (from Beyer and Roesler, 2008) .....	41
Table 27. Friction Testing Data .....	42
Table 28. Summary of CRS Data .....	44

# **CHAPTER 1. INTRODUCTION**

## **1.1 OVERVIEW**

The Illinois Department of Transportation (IDOT) has used predominantly recycled materials in unbound aggregate base and subbase layers. IDOT first used recycled concrete as aggregates in a stabilized surface course in two interstate projects in 1986 and 1987. Each of the projects was approximately eight centerline miles long and involved rehabilitating an existing stretch of the interstate. The first project was a continuously reinforced concrete pavement (CRCP) inlay on I-57 near Effingham, Illinois and the second project was an asphalt concrete pavement inlay south of Ullin, Illinois, also on I-57 (Van Matre and Schutzbach, 1989). The I-57 CRCP inlay is the only IDOT project that has used recycled concrete aggregate (RCA) in the concrete surface mixture.

The I-57 CRCP inlay project was carried out to replace a faulted jointed reinforced concrete pavement (JRCP) that contained high-quality aggregates that were not showing signs of D-cracking. The original JRCP was crushed using a jaw and roll crusher. The new CRCP structural design was a 10-in concrete surface and a 7-in cement stabilized base. The slab geometry, uniquely, included an 18-in widened lane, which was the first one in Illinois, but has not been widely used since. Both recycled coarse and fine aggregates were used in the concrete mixture. Fly ash and natural sands were also employed in the RCA concrete to improve the concrete workability. Periodic friction tests, ride quality tests, and condition surveys have been conducted over the years. A five-year evaluation of the I-57 CRCP inlay found no major problems (Schutzbach, 1993). Currently, the CRCP inlay is over 20 years old and is still providing service to approximately 17,000 ADT. However, this CRCP section is beginning to show some signs of deterioration due to settlement cracking, which has been attributed to the tube feeding process used during the original construction, and has manifested itself in other CRCP projects in the state such as sections of I-39 south of I-80 (Roesler et al., 2005). Due to the current distress level on this section, an asphalt concrete overlay is programmed to take place in the next couple of years.

## **1.2 RESEARCH OBJECTIVE**

The objective of this research was to summarize and document the 20-year structural and functional performance of the I-57 CRCP inlay that used recycled concrete as the primary coarse and fine aggregate. The performance of the CRCP inlay is compared with the performance of similarly aged and trafficked CRCP in the state of Illinois.

## **1.3 PROJECT TASKS**

The general objective of this study was to summarize the 20-year performance of the I-57 CRCP inlay. Accomplishing this objective required the following tasks to be completed:

- Task 1: A brief literature review to determine the current expected performance of rigid pavement containing RCA. Special emphasis was given to a recent

thesis (Sturtevant, 2007) which published field information from the I-57 CRCP inlay.

- Task 2: A structural evaluation of I-57 CRCP using distress surveys collected by IDOT. The distress data was analyzed to look at the distress development and deterioration rate of the section. The falling weight deflectometer (FWD) data was used to evaluate changes in the structural capacity of the section over time; e.g., maximum deflection, load transfer efficiency, and subgrade *k*-value, for both northbound and southbound lanes. IDOT video logs were reviewed to determine the average crack spacing of the sections and to check the number of distresses associated with loading; i.e., punchouts and patches.
- Task 3: A functional evaluation of I-57 CRCP using friction and IRI data collected by IDOT. The functional data was reviewed and analyzed in a time series to determine how the functional properties of the roadway had changed, and also how the structural deterioration affected the functional performance of the sections.
- Task 4: Conduct additional field-based data collections, if necessary. For this report, eight additional core samples were taken to evaluate the presence of alkali-silica reaction (ASR) or any other deleterious reaction. The results of these tests were important in determining if RCA has a long-term potential for ASR development.
- Task 5: Develop a final report summarizing the findings of Tasks 1 through 4.

## **CHAPTER 2. LITERATURE REVIEW**

### **2.1 PURPOSE OF LITERATURE REVIEW**

There have been numerous studies and projects on the use of RCA in concrete pavement applications. The following literature review has focused on providing a brief summary of the typical fresh and hardened concrete properties of RCA used in concrete pavement. Workability and air content are the fresh concrete properties that will be reviewed. Hardened properties such as durability, strength, modulus of elasticity, creep, and drying shrinkage will be discussed. A brief overview of the findings from an extensive field survey and laboratory study of recycled concrete pavements (Sturtevant, 2007) will be presented. Three recent studies reporting information from this experimental section of I-57 will also be reviewed. The first study was conducted by Sturtevant (2007) that looked at the overall performance of this section and how it compared with other RCA pavements in the United States. The second study by Roesler et al. (2003 and 2005) focused on explaining the excessive longitudinal cracking present within this section. The final study, completed by Peterson (2008), looked specifically at the air void system and whether there was deleterious ASR present.

### **2.2 RCA FRESH CONCRETE PROPERTIES**

#### **2.2.1 Workability**

The workability of concrete is affected by a number of factors which may include water content, aggregate type, size, shape, mixture proportions, and temperature. In the case of RCA, most studies show that RCA concrete exhibits a reduction in workability. The decrease in workability of concrete can be attributed to its higher aggregate angularity, surface texture, and absorption capacity for both coarse and fine RCA (Cuttell et al., 1997).

In considering aggregate angularity and surface texture, Snyder et al. (1994) suggest that, typically, coarse aggregates are not the significant problem but rather the fine RCA particles. The use of fine RCA greatly increases the harshness of the mixture because the angular fine particles replace the spherical river sands that are normally used.

Maintaining the design water content for a concrete mixture is one key for achieving good long-term performance of the particular concrete structure. Studies have shown that use of RCA requires additional water to achieve a similar level of workability as virgin aggregate concrete. This additional water is due to the high absorption and surface characteristics of the RCA material. The high absorption rate is primarily due to the more porous cement paste fraction attached to the crushed aggregate particles. It is generally accepted that concrete made using just RCA coarse material should need approximately 5 percent more water than similar concrete with virgin coarse aggregate. If both recycled concrete coarse and fine aggregates are used, then up to 15 percent additional free water is required to maintain the same level of workability.

The variation in the RCA absorption capacity can lead to changing water content demand, workability, and hardened concrete properties. To better control the variable water demand of RCA concrete due to the changing RCA absorption capacity, the Federal Highway Administration (FHWA, 2004) suggests keeping RCA stockpiles

saturated. This recommendation involves developing adequate procedures to ensure a consistent and uniform positive moisture content of the RCA. At a minimum, this means presoaking of the aggregate so that positive moisture content exists in the aggregate source (Snyder et al., 1994). The addition of excessive saturated surface dry (SSD) water for workability without a proportionate increase in cementitious content can lead to strength and durability issues. This extra cementitious content must be balanced with the economics of RCA versus virgin aggregate concrete.

As a way of maintaining workability and reasonable water-to-cement ratios, it is recommended that RCA fines be limited to 25 to 30 percent in addition to natural fine aggregates, water reducers, and/or fly ash pozzolans be used (Cuttell et al., 1997). The FHWA (2004) has recommended a limit of 20 percent RCA fines in the mixture.

### **2.2.2 Air Content**

The air contents of RCA concrete are generally higher and have greater variation at similar dosage rates than conventional concrete. Research conducted by Vandebossche and Snyder (1993) state that air content may be up to 0.6 percent higher than air contents in conventional concrete mixes. This behavior results from the higher porosity of the recycled aggregates themselves and from the entrained air in the original mortar fraction (Snyder et al., 1994).

## **2.3 HARDENED CONCRETE PROPERTIES**

### **2.3.1 Strength**

Researchers have primarily reported a reduction in strength when RCA is used as a substitute for virgin aggregates. The amount of strength reduction varies but can typically be between 2 to 10 percent. The main reasons for the strength reduction when using RCA are the following: higher air content with RCA; reduction in the amount of virgin or natural aggregate; higher porosity because of the porous mortar component of RCA; the resistance of RCA to mechanical action (which is lower than that of the corresponding virgin aggregate); and a higher proportion of interface transition zone areas in the concrete containing RCA, which include areas of interface between natural aggregate and mortar—both new and old—and also between the new and old mortars (Snyder et al., 1994). The FHWA (2004) has linked the strength reduction primarily to the addition of lower strength RCA fines (<2 mm).

The Cuttell et al. (1997) and Sturtevant (2007) studies on RCA concrete pavements demonstrated that all test sections increased in strength over time except one. Snyder et al. (1994) did report that researchers using lower water–cement ratios for concrete containing RCA can result in similar and sometimes higher strengths. This behavior was attributed to one or more of the following factors: the recycled PCC mixture used a lower water–cementitious ratio, or the use of approximately 25 percent recycled fine aggregates, or both. The 25 percent value was determined by a study conducted in Michigan by Fergus (1980). In his study, he varied the percentage of RCA fines to compare the flexural strength of concrete. The highest strength was obtained using approximately 25 percent recycled fines, with recycled concrete exceeding the control concrete when approximately 15 to 45 percent recycled fines were introduced.

### **2.3.2 Modulus of Elasticity**

The majority of research has shown that RCA lowers the modulus of elasticity. The lower elastic modulus of the RCA is the main reason for the reduction in the concrete elastic modulus. Snyder et al. (1994) reported that the elastic modulus of RCA concrete is typically 20 to 40 percent lower than conventional concrete, but the reduction would depend on the amount, type, and quality of RCA used. A reduced concrete modulus should not have significant effects on the concrete pavement fatigue resistance, but lower modulus values can increase pavement deflections.

### **2.3.3 Creep**

The compressive creep is higher for RCA concrete due to the larger paste component and may be 20 to 40 percent higher than conventional concrete pavements (Snyder et al., 1994). The increased compressive creep is a result of the presence of old mortar component on the recycled concrete coarse aggregate. One note is that compressive creep is not a major issue in concrete pavements, since tensile cracking is the primary mode of failure. Of greater interest would be the tensile creep characteristics of RCA concrete, which have not been reported by researchers.

### **2.3.4 Drying Shrinkage**

The use of RCA increases the drying shrinkage of concrete. This results from an increase in the total mortar content and a lower total aggregate volume (Cuttell et al., 1997). Studies show that no general trend exists to predict the magnitude of shrinkage. Snyder et al. (1994) reported difference in shrinkage between conventional and recycled concrete mixtures as low as 14 percent and as high as 95 percent. The key factor in the magnitude of the shrinkage was the volume of coarse and fine RCA present in the concrete mixture.

### **2.3.5 Coefficient of Thermal Expansion**

The average coefficient of thermal expansion for RCA concrete is generally higher than concrete made with virgin aggregates. This is attributed to the lower effective aggregate contents in RCA concrete, which offer less resistance to volumetric changes due to temperature movements.

### **2.3.6 Durability**

Snyder et al. (1994) has reported that durability of concrete containing RCA is generally equal to or better than that of virgin concrete. Cuttell et al. (1997), however, noted a lack of long-term durability monitoring and testing to confirm this conclusion. Durability will be further developed in the following sections of this study on D-cracking and alkali-silica reactive aggregates.

### 2.3.7 Aggregate Freeze–Thaw Durability

Durability cracking (D-cracking) is a series of closely spaced, crescent-shaped cracks on the concrete surface adjacent and parallel to joints and cracks. The primary D-cracking mechanism is internal freeze–thaw pressures generated within certain types and sizes of coarse aggregates. In using RCA with D-cracking susceptible aggregates, the major concern is the recurrence of D-cracking (Embacher, 1999).

Two methods have been shown to reduce the potential for D-cracking performance problems with RCA in pavements. These include reducing the aggregate size during the crushing operation and using fly ash as a partial replacement for cement (FHWA, 2004). With the first method, it has been shown that crushing a potential D-cracked aggregate into a smaller size will reduce the likelihood of D-cracking performance problems (FHWA, 2004). Snyder et al. (1994) suggested an aggregate top size of 0.75 in to reduce the magnitude of individual particle dilations. Laboratory research by Embacher (1999) demonstrated that even D-cracked concrete can pass the freeze–thaw standardized test (ASTM C666) if the RCA's maximum size was reduced below the critical size. With the second method, using fly ash as a cement replacement has been shown to greatly reduce D-cracking. This improved durability has been attributed in part to the improved workability of the fly ash concrete and use of less water, making the mixtures less permeable (Snyder et al., 1994). Cuttell et al. (1997) reported no recurrent D-cracking problems in the concrete pavement containing RCA that he surveyed.

### 2.3.8 Alkali-Silica Reactive Aggregates

Alkali-silica reaction (ASR) is caused by the reaction of certain forms of silica in the aggregates, alkalis in the cement paste, and readily available water. With the use of RCA, it is thought that RCA concrete is more susceptible to ASR than virgin aggregates. However, this is an area of research that still needs to be resolved and there is not overwhelming evidence that RCA have increased ASR in concrete pavement.

One researcher reports that if recycled concrete with ASR is used, it may be worse than the ASR in the original concrete (Sturtevant, 2007). The reason for this is that the new cement supplies more alkalis to the reaction that already exists. Snyder et al. (1994) warn that ASR may be increased in RCA because of the reduction in the aggregate size during the recycling process (there is more surface area for the reaction to take place).

There are many ASR mitigation techniques that are currently being used. Mitigation techniques recommended by Cuttell et al. (1997) and Snyder et al. (1994) include using low alkali cement (less than 0.6 percent  $\text{Na}_2\text{O}$  equivalent), blending the RCA with quality natural aggregates to reduce the number of reactive constituents, and using Class F fly ash.

One issue with ASR is accurately identifying the presence of deleterious ASR in the concrete pavement. Cuttell et al. (1997) and Sturtevant (2007) both used the uranyl acetate test to look for ASR in their research. This rapid test applies uranyl acetate to a concrete sample. If reactive silica is present in the sample, the uranyl acetate will be adsorbed into the surface of the silica and will glow neon green when exposed to ultraviolet light. Cuttell et al. (1997) cautions that results from the uranyl acetate test should be weighed with great care, as some researchers believe other constituents in

PCC materials besides alkalis will fluoresce when subjected to the uranyl acetate test. Furthermore, ASR gel can exist without being deleterious to the concrete.

## 2.4 Performance Summary of RCA in Concrete Pavements

An extensive field and laboratory study of concrete pavements containing RCA has recently been completed by Sturtevant (2007). This research conducted pavement surveys, field core extractions, and laboratory tests on 11 project locations covering 21 test sections (see Table 1), most of which were originally surveyed by a research team in the mid-1990s (Snyder et al., 1994; Wade et al., 1995; Cuttell et al., 1997). The original nine pavement sections included four jointed reinforced concrete pavement (JRCP), four jointed plain concrete pavement (JPCP) and one continuously reinforced concrete pavement (CRCP). A summary of the important design features of the 2006 survey are listed in Table 2. It should be noted that I-90 in Wisconsin (WI2) was the only other CRCP section containing RCA.

Table 1. Summary of RCA Concrete Pavement Site Locations (Sturtevant, 2007)

Project Location	Route	Site Title	Test Strip Location	Pavement Type
Waterbury, CT	I-84	CT1-1	WB, MP 33.71-33.91	Recycled
		CT1-2	EB, MP 33.94-33.83	Control
Rock Rapids, IA	U.S. 75	IA1-1	n/a	Recycled
		IA1-2	NB, Sta. 1091+00 – 1101+00	Recycled
Effingham, IL	I-57	IL1-1	NB, Sta. 5417+50 – 5427+50	Recycled
		IL1-2	SB, Sta. 5427+50 - 5417+50	Recycled
Johnson Co., KS	K-7	KS1-1	NB, .5 mi. north of 55 <sup>th</sup> St.	Recycled
		KS1-2	SB, 500' from KS River Bridge	Control
Brandon, MN	I-94	MN1-1	WB, MP 90.9-91.1	Recycled
		MN1-2	WB, MP 87.0-87.2	Control
Beaver Creek, MN	I-90	MN2-1	EB, Sta. 89+90 – 100+16	Recycled
		MN2-2	WB, Sta. 100+00 – 90+00	Recycled
Worthington, MN	US 59	MN3	SB, MP 27.00	Recycled
Zumbrota, MN	US 52	MN4-1	NB, Sta. 983+88 – 994+14	Recycled
		MN4-2	NB, Sta. 1035+01 – 1045+27	Control
Menomonie, WI	I-94	WI1-1	EB, MP 39.6-39.8	Recycled
		WI1-2	EB, MP 40.1-40.3	Recycled
Beloit, WI	I-90	WI2-1	WB, MP 176.8-177.0	Recycled
		WI2-2	WB, MP 176.2-176.4	Recycled
Pine Bluffs, WY	I-80	WY1-1	EB, starts 130' ft. east of MP 400	Recycled
		WY1-2	WB, ends 159' W of WY-NE Border	Control

Sturtevant (2007) found that the concrete pavements containing RCA were, overall, performing in a manner similar to the control sections. Several RCA sections had a higher occurrence of longitudinal cracking, transverse joint deterioration, and slightly more transverse cracks. The increases in some of these distresses were postulated to be a result of higher mortar content, lower maximum size aggregate, and deleterious ASR developing in the concrete. Even though 10 of the 16 sections indicated the presence of ASR (from uranyl acetate and petrographic analysis - ASTM C 856;

modified ASTM 1293), they still consistently performed the same relative to the control sections. Based on Sturtevant's findings, proposals for RCA concrete pavement should first carefully evaluate ASR potential of certain cement, pozzolan, and RCA combinations; evaluate D-cracking potential; minimize mortar content, especially in the crushing of the old concrete pavement; maximize the size of the coarse RCA; and provide good load transfer across joints.

Table 2. Summary of RCA Concrete Pavement Features (Sturtevant, 2007)

Site Title	Joint Spacing (m)	Slab (cm)	Dowel Diameter (mm)	Agg. Top Size (mm)	RCA Fines (%)	w/cm	Base** (cm)	Shoulder Type
CT1-1	12	23	38 (I-beam)	38	20	0.4	25	AC
CT1-2	12	23	38 (I-beam)	51	0	0.45	25 and 46	AC
IA1-1	6.1	23	None	38	16	0.54	15	PCC
IA1-2	6.1	23	None	38	30	0.54	15	PCC
IL1-1	CRCP	25	n/a	38	35	0.37*	18	AC
IL1-2	CRCP	25	n/a	38	36	0.40*	18	AC
KS1-1	4.7	23	None	19	25	0.41	10 CTB	AC
KS1-2	4.7	23	None	38	0	0.41	10 CTB	AC
MN1-1	8.2	28	32	19	0	0.47	15	AC
MN1-2	8.2	28	32	19	0	n/a	15	AC
MN2-1	8.2	23	25	19	0	0.46	8	AC
MN2-2	8.2	23	25	19	0	0.46	8	AC
MN3	4.0-4.9-4.3-5.8	20	None	19	0	0.44	3	AC
MN4-1	8.2	23	25	38	0	0.44	13	AC
MN4-2	8.2	23	25	25	0	0.47	13	AC
WI1-1	3.7-4.0-5.8-5.5	28	None	38	0	n/a	15 over 23	PCC
WI1-2	3.7-4.0-5.8-5.5	28	35	38	0	n/a	15 over 23	PCC
WI2-1	CRCP	25	n/a	38	0	n/a	15 over 23	PCC
WI2-2	CRCP	25	n/a	38	0	n/a	15 over 23	PCC
WY1-1	4.3-4.9-4.0-3.7	25	None	38	22	0.38	10	PCC
WY1-2	4.3-4.9-4.0-3.7	25	None	25	0	0.44	n/a	PCC

Note: \* Water/(Cement + Fly Ash) Ratio

\*\* Aggregate base unless otherwise specified

## CHAPTER 3. I-57 RECYCLED CRCP PROJECT SUMMARY

### 3.1 OVERVIEW

In April 1986, IDOT began the reconstruction of a section of I-57 as a demonstration project to evaluate the viability of recycling PCC pavements into a new concrete pavement. The following sections provide a summary of the background information of this experimental recycled concrete pavement, which has been reported previously by Van Matre and Schutzbach (1989) and Schutzbach (1993).

### 3.2 GENERAL INFORMATION

The project is located on I-57 just north of Effingham, IL between mileposts 164.2 and 168.3. The entire project was constructed as a continuously reinforced concrete

pavement (CRCP) in two phases. The northbound lanes were the first constructed from April 1 to November 1, 1986. The southbound lanes were constructed from April 1 to November 1, 1987. All lanes were open for traffic between November 1, 1986 and April 1, 1987, respectively.

### 3.3 PREVIOUS JRC PAVEMENT SECTION

The new concrete pavement with RCA was designed to replace a 10-in-thick JRC pavement with 100-ft joint spacing built in 1964. The JRC was placed on top of a 6-in aggregate subbase layer, as shown in Figure 1. In 1978, the 8-in bituminous shoulders were reconstructed, along with the installation of underdrains.

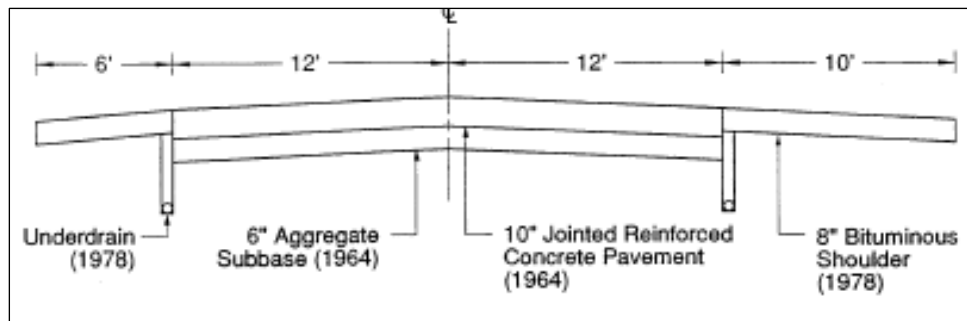


Figure 1. Original pavement cross section (Schutzbach, 1993)

The original JRC pavement section did not show any signs of D-cracking which was prevalent on many distressed concrete pavements in Illinois. However, two to three transverse cracks existed per slab panel. These cracks and most of the joints were badly faulted and spalled. The shoulders and underdrains were still in excellent condition at the time of reconstruction.

### 3.4 STRUCTURAL DESIGN OF CRCP INLAY

During the design phase of the recycled CRCP in 1984, the average daily traffic was 10,000 vehicles with 2,000 trucks. A 20-year design life was selected for the traffic estimation and material specifications. An inlay was specified because of the excellent condition of the existing shoulders and underdrains. The final design was a 27-ft-wide, 10-in-thick CRC pavement on a 7-in cement-stabilized subbase, as seen in Figure 2. The subbase was designed 3 in higher than the standard IDOT subbase to allow for a crown change and because of a desire to have stabilized materials in place over the subgrade.

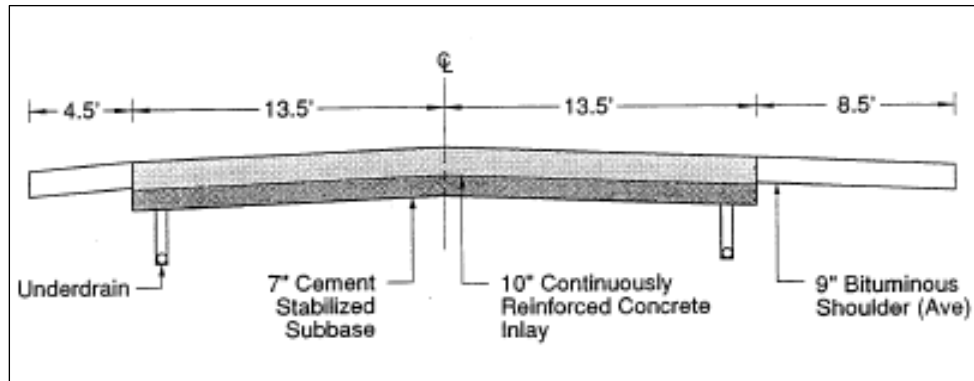


Figure 2. Cross section of I-57 CRC pavement inlay with RCA (Schutzbach, 1993)

Several unique features of this project were the 1.5-ft extended (widened) lane and the use of RCA as the primary aggregate source for the surface concrete mixtures. RCA has not been used subsequently and widened lanes only infrequently. The amount of longitudinal reinforcing steel was 0.7 percent. Longitudinal reinforcing steel was #7 without epoxy coating placed on 8-5/8 inch centers. The longitudinal contraction joint was tied together with 30-in-long #5 bars placed at 2.5-ft centers.

### 3.5 PAVEMENT MATERIALS

Table 3 shows the crushed concrete aggregate gradation. Modifications to the standard IDOT gradations CA-07 and FA-07, similar to AASHTO M43 size 57 and AASHTO M6, were used to allow for the use of RCA fines. No additional quality standards were set for the crushed concrete aggregate over existing virgin aggregates. The RCA did meet the 1-in nominal maximum size freeze-thaw requirement and the Los Angeles abrasion and deleterious material requirements. However, the RCA did fail IDOT's sodium sulfate soundness test (AASHTO T104), which has been an indicator of aggregate weathering capability. It was postulated that the sodium sulfate test failed because of the reaction with the concrete mortar; thus, the sodium sulfate quality requirement was waived (Schutzbach, 1993). The National Stone Association (NSA) has indicated that the sodium sulfate test has a poor correlation with freeze-thaw resistance of the aggregate (NSA, 1991). IDOT should continue to rely on its freeze-thaw test for RCA because the sodium sulfate test may give erroneous results. The results of IDOT's original material tests can be seen in Table 4.

The other main durability issue was whether the existing chloride content of the RCA (0.181 to 0.186 percent by weight of cementitious content) was high enough to activate and/or accelerate corrosion in the new CRCP-containing black steel and RCA. IDOT went ahead with non-epoxy coated steel primarily for economic reasons, since research on critical chloride content suggested that the measured values were within acceptable ranges at the time. Bentur et al. (1997) note that most specifications which included chloride limits state that it should be less than 0.2 percent by weight of cementitious content. Chloride content between 0.2 and 0.4 percent presents some risk, while 1 percent content is considered high risk for steel corrosion. Research has also demonstrated that the corrosion rate of steel embedded in concrete is very low if the chloride content is less than 0.5 percent (Bentur et al., 1997). The current ACI 201 (1994) limits chloride content to 0.10 percent for reinforced concrete structures exposed to chlorides, and 0.15 percent for structures not exposed to external chlorides. To address

the current ACI chloride content limit, IDOT would need to blend RCA with virgin coarse aggregates. The petrographic examination shown in Appendix A, however, noted that the steel reinforcement was found to be in good condition without corrosion.

Table 3. I-57 Recycled Concrete Aggregate Gradations (Schutzbach, 1993)

PERCENT PASSING GIVEN SIEVE SIZE									
	1.5"	1"	1/2"	3/8"	#4	#16	#50	#100	#200
<b>Coarse Aggregate</b>									
Special Provision	100	90-100	30-60		0-10				0-2.5
1986 Test Results (59 tests)	100	93	37		8				1.5
1987 Test Results (39 tests)	100	91.5	34		7				1.1
<b>Fine Aggregate</b>									
Special Provision				100	94-100	45-85	3-29	0-10	0-6
1986 Test Results (63 tests)				100	100	49	14	6	4.8
1987 Test Results (37 tests)				100	100	48	13	5	3.7

Table 4. Recycled Concrete Aggregate Quality Tests (Schutzbach, 1993)

Aggregate	Freeze-Thaw	Sodium Sulfate Soundness, % Loss	Los Angeles Abrasion, % Loss	Deleterious Material, % of Sample	Absorption, %	Specific Gravity, Saturated Surface Dry (SSD)
CM-07	1" Max.	25	33	0.2	5.3	2.42
	-Meets criteria of 0.060% maximum expansion at 350 cycles	-Criteria of 15% maximum loss waived	-Meets criteria of 45% maximum loss	-Meets criteria of 5% maximum total deleterious		
FM-01	---	19	---	---	6.6	2.41
		-Criteria of 10% maximum loss waived				
---Denotes No Specification For Fine Aggregate						

### 3.6 CONCRETE MIXTURE DESIGN

Table 5 and Table 6 demonstrate the mixture design used for both the northbound and southbound lanes on I-57. IDOT required the use of 125 lb/yd<sup>3</sup> of Type C fly ash in the initial mixture design with the addition of up to 20 percent natural sand to improve workability, if necessary. With the high angularity of the crushed concrete aggregates, the initial mixture was harsh, with poor workability and an additional 25 lb/yd<sup>3</sup> of fly ash was added. The mixture design for Year 2 of the project (1987) was

changed to further improve the workability of the mixture and to balance out the stockpiled crushed concrete aggregate quantities.

Table 5. 1986 Concrete Mixture Design (Schutzbach, 1993)

INGREDIENT	QUANTITY, POUNDS	
	INITIAL DESIGN	REVISED DESIGN
Cement	515	515
Fly Ash	125	150
Recycled CM-07(SSD)(1)	1,721	1,818
Recycled FM-01 (SSD)	369	312
Virgin FA-01 (SSD)	554	570
Water (Includes water reducer and air-entraining agent)	282	249
<b>Total, Pounds/Cubic Yard</b>	<b>3,566</b>	<b>3,614</b>
Mortar Factor = $\frac{\text{Vol. mortar}}{\text{Vol. dry rodded aggregate}}$	0.80	0.72
Water/(Cement + Ash) Ratio	0.44	0.37
FM-01/CM-07 Recycled Use Ratio	0.21	0.17
Fineness Modulus (ASTM C 33-85)	3.1	3.0

(1) (SSD) Denotes Saturated Surface Dry Condition

Table 6. 1987 Mix Design Quantities (Schutzbach, 1993)

INGREDIENT	QUANTITY, POUNDS
Cement	515
Fly Ash	150
Recycled CM-07 (SSD)(1)	1,789
Recycled FM-01 (SSD)	312
Virgin FA-01 (SSD)	554
Water (includes water reducer and air-entraining agent)	266
<b>Total</b>	<b>3,586 Pounds/Cubic Yard</b>
Mortar Factor = $\frac{\text{Volume Mortar}}{\text{Vol. dry rodded aggregate}}$	0.74
Water/(Cement + Ash) Ratio	0.40
FM-01/CM-07 Use Ratio	0.17
Fineness Modulus (ASTM C 33-85)	3.0

(1) (SSD) Denotes Saturated Surface Dry Condition

### 3.7 CONSTRUCTION METHODS

Specific details about the construction of this section are contained in a paper by Van Matre and Schutzbach (1989). The referenced paper discusses in detail the preliminary work necessary, which included establishing a haul road, the JRC pavement breaking and crushing procedures, and the paving operations. This section will only highlight subbase stabilization and reinforcement placement.

### **3.7.1 Subbase Stabilization**

Illinois requires all interstate concrete pavements to be placed over a stabilized base/subbase. The subbase on the northbound lanes was a 27-ft-wide, mixed-in-place cement–aggregate subbase. Two in of gravel were added to the existing aggregate subbase to establish a new profile. Cement was blown onto the grade from a tanker during three passes, with a required cement content of 7.6 percent by volume of aggregate.

On the northbound lanes, the cement-stabilized subbase was constructed 27 ft wide. A 1500-ft test section was constructed in 1986 to determine if a 24-ft-width subbase would be sufficient. Based on visual inspection from November 1986 to April 1987, it was determined that both the 24-ft test section and the 27-ft control section were comparable. It was decided to only stabilize the southbound subbase to a width of 24 ft to provide a less obstructed path to the underdrains and to prevent possible damage to the underdrains. The southbound lanes also had 2 in of RCA instead of gravel mixed with the subbase before stabilization.

### **3.7.2 Steel Reinforcement Placement**

The longitudinal reinforcing steel was placed using the tube feeding method. This method is no longer used by IDOT due to problems with inadequate cover depth, and more recently, the discovery of its link to the longitudinal (settlement) cracking on various CRCP sections in Illinois (Roesler et al., 2005).

## **3.8 FRESH CONCRETE PROPERTIES**

The recycled concrete mixture was required to meet standard specifications for slump, air content, and strength. The average slump was 2 in, air content was over 6 percent, 14-day compressive strength exceeded 3500 psi, and the 14-day flexural strength was approximately 850 psi.

## **3.9 TRAFFIC LOADINGS**

As stated previously, the ADT in 1984 was 10,000 vehicles with 2,000 trucks. In 1988, the first full year that both I-57 sections were open, the ADT was reported to be 11,500 with 2,600 trucks. Throughout the life of the pavement, ADT surveys were conducted every year, with truck class surveys being conducted once every 4 years, prior to year 2000. Table 7 shows the traffic history and the estimated equivalent single-axle loads (ESALs) in the design lane.

Table 7. I-57 Traffic History and Estimated ESALs in Design Lane

Year	ADT	PV	Single Unit Trucks	Multiple Unit Trucks	Estimated Annual ESALs (millions)
2008	16300*	10000*	700*	5600*	1.80
2007	16300*	10000*	700*	5600*	1.80
2006	16300	10000	700	5600	1.80
2005	17300	11350	750	5200	1.68
2004	17100	11300	900	4900	1.59
2003	18300	13100	600	4600	1.48
2002	15300	10400	600	4300	1.39
2001	14700	9200	800	4700	1.53
2000	17400	11600	600	5200	1.67
1999	17400	11832*	522*	5046*	1.62
1998	17800	12764*	490*	4673*	1.50
1997	17200	12728*	430*	4042*	1.30
1996	16800	13000	400	3400	1.09
1995	15900	12164*	398*	3339*	1.07
1994	15200	11476*	380*	3344*	1.07
1993	14500	10875*	363*	3270*	1.05
1992	12700	9400	400	2900	0.94
1991	12400	9300*	372*	2728*	0.88
1990	12700	9525*	381*	2794*	0.90
1989	11800	9027*	295*	2478*	0.80
1988	11500	8900	300	2300	0.74
1987	11000	8470*	330*	2200*	0.71
1986	10900	8393*	327*	2180*	0.70
<b>Total</b>					<b>29.1</b>
<i>* Denotes estimated value</i>					

Annual ESALs for each year were computed using the IDOT formula from Chapter 54 of the *BDE Manual* (2002):

$$\text{Annual ESALs} = [(0.15 * PV * P) + (143.81 * SU * S) + (692.42 * MU * M)]$$

where,

PV = the average daily number of passenger vehicles in all lanes for both directions;

P = the passenger car lane design lane distribution factor;

SU = the average daily number of single-unit trucks per day in all lanes for both directions;

S = the single-units truck design lane distribution factor;

MU = the average daily trucks per day for all lanes in two directions; and

M = the multiple-unit truck design lane distribution factor.

For four-lane facilities, IDOT has previously determined the distributions factors (P, S, and M) to be 0.32 for passenger vehicles, 0.45 for single-unit trucks, and 0.45 for multiple-unit trucks. In Table 7, the numbers with asterisks for 2007 and 2008 have been estimated to calculate the total number of ESALS in the design lane through 2008. It is estimated that this section of pavement has carried 29.1 million ESALS of traffic in the design lane over its service life.

## CHAPTER 4. PREVIOUS I-57 CRCP RESEARCH

This section will review three studies that have been recently completed on the I-57 recycled concrete CRCP section. The first study was conducted by Sturtevant (2007) as part of his master's thesis on the performance of multiple sections of RCA pavement throughout the U.S. The second and third studies were conducted, respectively, by Roesler et al. (2003, 2005) and Peterson (2008), to investigate the cause of longitudinal cracking occurring on the I-57 inlay and several other CRCP sections in Illinois.

### 4.1 RECYCLED MATERIALS RESOURCE CENTER SURVEY

Sturtevant (2007), in conjunction with the Recycled Materials Resource Center (RMRC) at the University of New Hampshire, conducted both field and laboratory testing on 11 recycled concrete pavement sites throughout the United States (21 test sections). The main focus of this project was to document the performance of rigid pavements containing RCA. His work revisited nine sections originally tested by Cuttell et al. (1997) and included two new sections, one of which was the I-57 recycled concrete CRCP section. A summary of Sturtevant's collected data for each direction of the I-57 section is shown in Table 8, along with the average values obtained from his recycled concrete pavement and control section surveys. IL1-1 represents the northbound section and IL1-2 represented the southbound section.

Table 8. I-57 Field and Laboratory Performance Data and Average RCA and Control Pavement Performance Data (after Sturtevant, 2007)

Test and Value	IL 1-1 (RCA 1) NB	IL 1-2 (RCA 2) SB	2007 Average RCA	2007 Average Control
Aggregate Top Size, mm	38	38	32	32
Recycled Fines, %	35	36	12	0
Longitudinal Joint Seal Damage, m/km	1000 (100%)	1000 (100%)	997 (99%)	1000 (100%)
D-cracking, % Slabs	100	47	13%	0%
Pumping, % Slabs	0	0	0%	0%
Slab/Patch Deterioration, % Slabs	0	0	1%	0%
Avg. Lane to Shoulder Drop off, mm	n/a	8	13	21
Avg. Lane to Shoulder Separation, mm	3	12	6	10
Longitudinal Cracking, m/km	1252	527	326	2
Deteriorated Transverse Cracks/km	0	n/a	52	7
Total Transverse Cracks/km	0	59	58	17
Split Tensile Strength, MPa	1.9	3.6	3.1	3.1
Compressive Strength, MPa	56.0	55.2	48.0	47.5
Uranyl Acetate Reaction	High	High	Low	None
Modified ASTM 1293, % Expansion at 108 Days	0.345	0.166	0.257	0.167
Young's Modulus, GPa	29.1	26.7	28.4	34.1

Comparing the I-57 test data with average RCA pavements, a couple of noticeable differences exist such as the amount of recycled fine aggregate content, the presence of D-cracking, total transverse cracks per km, tensile strength, longitudinal cracking, and uranyl acetate reaction. Typically, the recycled concrete is only used as a coarse aggregate in surface concrete. The amount of RCA used as fine aggregates for the Illinois project was quite high, but this does not appear to be linked with any negative performance indicator on this section. Sturtevant (2007) listed D-cracking as occurring 100 percent of the time on the northbound section, which has never been reported by IDOT in any of their past surveys and is an error. The current IDOT video survey in 2007, and a 2008 University of Illinois visual survey did not detect any D-cracking on the northbound or southbound sections, nor was it present on the original JRCP (Schutzbach, 1993). There is a significant amount of longitudinal cracking on I-57, which will be thoroughly discussed in the next section.

The total transverse cracks per km listed in Table 8 is misleading, since CRCP has average transverse crack spacing between 1 and 2 m. Therefore, the report of zero transverse cracks on the northbound and only 59 on the southbound is erroneous data. The split tensile strength was very low relative to the results reported by Roesler et al. (2003), which had a minimum tensile strength of 5 MPa. This lower tensile strength may be a result of some of the longitudinal hairline cracks on the surface affecting the split tensile strength.

Alkali silica reactivity (ASR) was suspected due to the positive results from the uranyl acetate test (Figure 3), a modified ASTM C1293 test (Figure 4), and petrographic analysis of the cores under a stereo microscope (Figure 5). This is contrary to a petrography study of several I-39 and I-57 cores done by Construction Technology Laboratories, Inc. for the Roesler and Ulreich (2002) study, which showed no deleterious reactions, such as ASR, were present. Due to several discrepancies between the work of Sturtevant (2007) and previous studies on this I-57 section on D-cracking, CRCP transverse cracking, and ASR, the validity of some of the data reported by Sturtevant for this section is somewhat questionable. Further cores were extracted from I-57 in 2008 to conduct another independent petrographic analysis for ASR. The results are discussed later in this report in section 4.2.3.

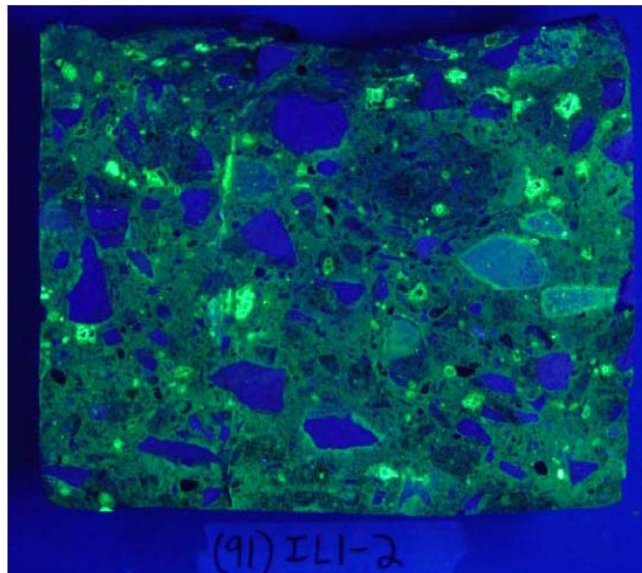


Figure 3. I-57 fractured core under ultra-violet light and coated with uranyl acetate dihydrate (Sturtevant, 1997)

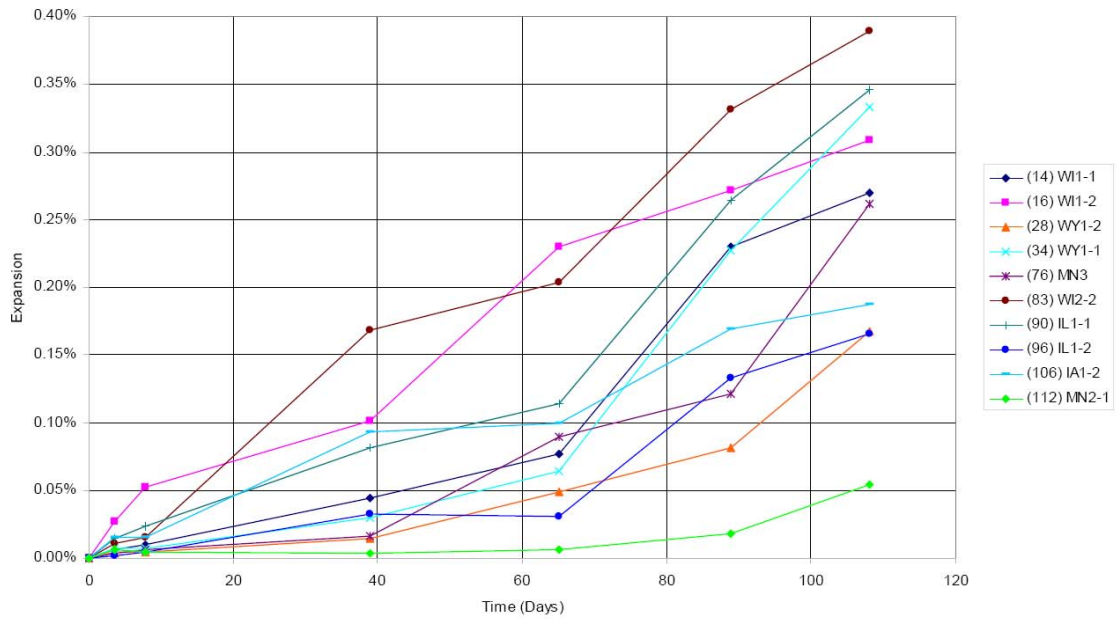


Figure 4. Expansion versus time for modified mortar bar expansion – ASTM C1293 (Sturtevant, 2007)



Figure 5. Photo of void filled with ASR gel from Illinois CRCP test section (Sturtevant, 2007)

## **4.2 ILLINOIS LONGITUDINAL CRACKING INVESTIGATION**

Earlier tests conducted by IDOT District 7 (1998) came to a preliminary conclusion that corrosion of the unprotected rebar may be the primary factor in producing the longitudinal cracking. In 2001 and 2002, investigations into longitudinal cracking distress on CRCP pavement were conducted focusing on the key similarities between the sections showing longitudinal cracking: non-epoxy coated steel reinforcement, tube feeding of the steel during construction of the pavement, and the presence of corrosion products on the steel near the longitudinal cracks. Sections from the I-57 CRCP were also recently examined by Roesler et al. (2003) to determine the cause of unknown longitudinal cracks. Visual surveys, petrographic examination, strength, density, and several nondestructive evaluation procedures were run to characterize the quality of the concrete and the position and condition of the reinforcing steel. A petrographic examination was also initiated as part of this research in collaboration with Dr. Karl Peterson of Michigan Technological University (Peterson, 2008) to re-evaluate the findings of Sturtevant (2007), which indicated that extensive deleterious ASR was one source of the observed cracking. A summary of the results of the various studies are below.

### **4.2.1 Field Survey and Coring (2002)**

A thorough field investigation of the longitudinal cracking distress on I-57 and several I-39 sections was conducted by Roesler and Ulreich (2002) for the IDOT. Fourteen cores were taken from the recycled CRCP section on I-57 that exhibited the longitudinal cracking distress, with six containing steel reinforcement. The longitudinal cracking corresponded to the underlying reinforcement, since only one core taken over a longitudinal crack failed to include steel in the core. The depth of the steel ranged from 3 to 6 in for the 10-in thick CRC pavement. The amount of corrosion present on the reinforcement did not seem to correspond with the amount of cover. No conclusive evidence could be found from these cores that could determine the possible cause for the longitudinal cracking distress. Roesler and Ulreich (2002) also dismissed ASR or D-cracking as possible explanations for the cracking based on their visual observation of the surface cracking. Furthermore, a petrographic analysis of one core from I-57 by Construction Technology Laboratories Inc. (Vollmer, 2002) concluded that the concrete quality was consistently good throughout and no conclusive cause could be determined from the petrographic analysis for the longitudinal distress condition.

Previous to this study, eight cores were taken by District 7 personnel on March 26, 1998 to determine the cause of the longitudinal cracking. In the District 7 report, the most significant observation was the corrosion around the rebar. Seven of the eight cores had visual confirmation of corrosion. Initially, the correlation between the District 7 data, petrographic analysis comments, and I-39 cores helped the District reach the preliminary conclusion that corrosion of the unprotected rebar may be the primary factor in producing the longitudinal cracks.

### **4.2.2 Laboratory Investigation of CRC Field Slabs (2003)**

As a result of the initial field investigation and coring plan, tests were conducted on several full-scale (4 ft by 6 ft) slabs that were extracted from the I-57 recycled CRCP

section as a result of premature slab failure (Roesler et al. 2003, 2005). Three of the extracted slabs exhibited longitudinal cracking over the reinforcement bars and one of the slabs showed only minor longitudinal cracking. There were three main laboratory components carried out on the field slabs. The first was to visually inspect the concrete slabs to identify crack locations and the actual cover depth and center-to-center spacing of the rebar. The second part was to determine the depth of internal cracking and strength of the concrete at cracked and uncracked locations in each slab. The last phase was corrosion testing of the reinforcement bar.

Results of the visual analysis showed that the majority of cracks were located above and aligned with the longitudinal rebar, and were not influenced by the transverse cracks in the pavement. It also showed that all embedded longitudinal bars had suitable and consistent spacing with varying cover depths of 3.5 to 5.5 in. Longitudinal surface crack widths ranged from 0.01 to 0.05 in and transverse crack surface widths ranged from 0.016 to 0.06 in.

Results for the laboratory core testing showed that cores were uniform without segregation and had little or no evidence of rebar corrosion. There typically was a strong bond between the rebar and cement matrix without the presence of entrapped air below the bar. Compressive strength tests found good-quality concrete at the top (5211 to 5867 psi) and bottom (5211 to 7720 psi) of the slab, with the top half of the cores having lower strengths. Corrosion tests on the steel reinforcing bars showed very low corrosion potential for the in-place bars.

The study by Roesler et al (2003, 2005) concluded that longitudinal cracking was not caused by corrosion of the embedded steel reinforcing bars. It was hypothesized—and subsequently supported by the data—that the cause of the longitudinal cracking was a result of the tube feeding process during the original placement of the CRCP section. This occurred due to the lifting and subsequent settlement of the rebar during the concrete casting. This explanation fit well with the field and laboratory observations from both I-39 and I-57. Roesler et al. (2005) speculated that if the steel was originally placed at a 3.5-in depth from the surface, then it should still be at that position. However, it was found that the cover depth varied from 3.5 to 5.5 in, which supports the settlement-of-the-bars hypothesis. The change in specification to #7 bars in CRCP, which are 33 and 100 percent heavier per foot, respectively, than #6 and #5 bars could easily cause settlement in slip-formed concrete. In addition, CRCP pavement cast with reinforcing steel on chairs (IDOT District 1) did not exhibit any of the characteristic longitudinal cracking seen on I-39 and I-57. Finally, the use of recycled concrete would tend to exacerbate this phenomenon due to its lower bulk density.

#### **4.2.3 Petrographic Examination of CRCP Field Cores (Peterson, 2008)**

The visual evaluation of the CRCP inlay on I-57 near Effingham, Illinois with recycled concrete has continually raised questions whether the concrete is suffering from a materials-related distress, specifically alkali-silica reactivity (ASR) or D-cracking. At New Hampshire's Recycled Materials Resource Center (RMRC), Sturtevant (2007) had extracted and tested several cores from this I-57 project. He conducted several uranyl acetate tests, a modified ASTM C1293 expansion test, and a petrographic analysis of these cores to determine if ASR was present. He found that ASR was present and likely causing deleterious cracking. The objective of including this petrographic examination in this research study was to have an independent, qualified

examiner assess whether deleterious ASR or other mechanisms exist, in order to make an accurate assessment of the performance of this recycled concrete pavement.

IDOT personnel extracted eight cores from the northbound and southbound lanes (see Table 9) in similar locations to where the cores were taken for the Sturtevant study (2007). Four cores were sent to Dr. Karl Peterson at Michigan Technological University (MTU) for petrographic examination, specifically ASR and air void analysis.

Table 9. Location and Nomenclature for Extracted CRCP Cores

Core Designation	Lane	Station
NB1	North	5420+60
NB2	North	5422+50
NB3	North	5422+84
NB4	North	5424+58
SB1	South	5424+38
SB2	South	5422+57
SB3	South	5422+35
SB4	South	5420+40

The report of the results of this examination is presented in Appendix A and is summarized next.

The petrographic examination concluded that the cracks from the surface were not a result of deleterious chemical reaction and likely resulted from drying shrinkage. The carbonation depth of 0.25 in is slightly greater than normally expected for a concrete pavement. Carbonation depths on the order of 0.1 in are more common. This carbonation depth suggests that the hardened cement paste might be slightly more permeable than a normal concrete pavement, although the extensive surface cracking probably enhanced the depth of carbonation.

Polished slabs made from the cores were treated with sodium cobaltinitrite which turns potassium-bearing alkali-silica gels yellow. The carbonate coarse aggregate also picked up the yellow stain, but potassium-bearing clay minerals can also pick up the yellow stain. Although there were some alkali-silica reactions present in the coarse aggregate particles (yellow stain), it has not resulted in expansion cracking. For the most part, reactive fine aggregate particles did not exhibit any signs of cracking or expansion. In only two instances was cracking observed in a reactive fine aggregate particle. These cracks were limited to the fine aggregate particle and did not crack the surrounding cement paste matrix.

The entrained air properties appeared to be sufficient for freeze-thaw durability, with spacing factors in the range of 0.106 to 0.143 mm (less than the maximum recommendation of 0.2 mm) and specific surface values between 25.6 to 32.5 mm<sup>-1</sup>, which is greater than the minimum of 25 mm<sup>-1</sup>. The air void system was definitively ruled out as causing the surface cracking.

Based on the petrographic examination and previous studies, it is highly improbable that the cracking in the concrete is due to frost damage or alkali-silica reactions. The fact that ASR gel is present without any deleterious expansion and a normal air void system further justifies this conclusion. As stated in the previous sections, the likely cause of the longitudinal cracking is the excessive drying shrinkage, the presence of reinforcing bars, and settlement of the bars during the tube feeding process at the time of the original construction.

## CHAPTER 5. STRUCTURAL EVALUATION

Over the past 20 years, IDOT has collected distress surveys and conducted FWD tests on the I-57 CRCP inlay sections. This chapter will summarize the data to better quantify the structural performance of the CRC pavement containing RCA. Specifically, the FWD data collected over time will be used to evaluate the normalized deflections, transverse crack load transfer efficiencies (LTE), concrete elastic modulus, soil *k*-value, and subgrade resilient modulus. Visual distress data will be examined to look at the identified distresses associated with the pavement, such as longitudinal cracking, popouts, punchouts, and localized distress. Finally, the average crack spacing will be reported based on a 500-ft sampling near each milepost along the test section.

### 5.1 FALLING WEIGHT DEFLECTION (FWD) DATA

Deflection testing was conducted periodically using IDOT's Dynatest 8002 FWD. The FWD is a non-destructive testing device which simulates a moving wheel load on the pavement. Data analyzed include deflection at the center of the driving lane between transverse cracks (CN), leave crack of the outer wheel path (LC-OWP), leave crack at the edge of pavement (LC-Edge), and the true edge of the 13.5-ft lane (TE). All four locations were tested until 1995. In 1997, the center of the driving lane, leave crack in the outer wheel path, and leave crack at the edge were tested. After 1997, only three locations were tested: the center of the driving lane, outer wheel path, and true edge. Tests conducted in 1999 and beyond used only a single 9-kip drop, while tests conducted before 1999 used three drops: 4, 8, and 12 kips. Table 10 summarizes the FWD testing conducted for these test sections.

Table 10. FWD Testing Dates and Locations

Date	Direction	Drops	Location
May-06	NB, SB	1	CN, LC-OWP, TE
Aug-01	NB, SB	1	CN, LC-OWP, TE
Aug-99	NB, SB	1	CN, LC-OWP, TE
Apr-97	NB, SB	3	CN, LC-OWP, LC-Edge
May-95	NB, SB	3	CN, TE, LC-OWP, LC-Edge
Apr-90	NB, SB	3	CN, LC-OWP, LC-Edge, TE
Aug-89	NB, SB	3	CN, LC-OWP, LC-Edge, TE
Mar-89	NB, SB	3	CN, LC-OWP, LC-Edge, TE
Sep-88	NB	3	CN, LC-OWP, LC-Edge, TE
Jul-88	SB	3	CN, LC-OWP, LC-Edge, TE
CN = center of driving lane LC-OWP = leave crack outer wheel path TE = true edge LC-Edge = leave crack edge of pavement			

### 5.1.1 Deflection and Deflection AREA

The maximum deflection under the plate load (D0) was normalized to reflect a standard 9,000-lb load. The normalized deflections are given in mils (1 mil = 0.001 in). The deflection data presented are averages for the entire section for the year. The data for the center of the lane testing is shown in Table 11 and Table 12. Figure 6 graphically depicts the deflection over the life of the pavement. The mean normalized deflection ranged from 3.1 to 4.2 mils for the northbound direction and 3.0 to 4.0 mils for the southbound direction. In Figure 6, the 9-kip normalized deflections suggest an excellent structural support.

The deflection basin AREA term is calculated by the following formula:

$$\text{AREA (in)} = 6 * \left( 1 + 2 \frac{D1}{D0} + 2 \frac{D2}{D0} + \frac{D3}{D0} \right)$$

where D0, D1, D2, D3 are deflections at a distance of 0, 12, 24, 36 inches from the drop location. The AREA is determined in inches and has a maximum value of 36 in. The AREA communicates the ability of the pavement system to distribute the load out and is the main indicator of the pavement's structural integrity. The higher the AREA term, the more resistant the pavement system is to loading. The AREA data is summarized for the center of the driving lane in Table 11, Table 12, and Figure 7. The AREA for the northbound direction ranged from 30.2 to 31.1 in, while the southbound was between 30.5 to 31.1 in. The AREA term magnitude and consistency over time indicate excellent structural condition.

Table 11. Northbound Center Panel Averages for Deflection and AREA

Date	Direction	Pav Temp (°F) at 4in	No. of Tests	D0 (MILS)	D0 COV (%)	AREA (in)	AREA COV (%)
5/30/2006	NB	88	22	3.9	14.1	31.0	2.4
8/21/2001	NB	88	31	4.1	19.5	30.8	2.0
8/25/1999	NB	78	34	4.1	32.6	30.6	4.4
4/29/1997	NB	N/A	105	4.2	18.9	30.8	2.1
5/15/1995	NB	76	38	4.2	21.8	31.1	2.5
4/17/1990	NB	35	111	3.4	18.1	30.2	3.0
8/29/1989	NB	80	36	3.8	26.4	30.7	2.9
3/29/1989	NB	51	98	3.1	16.6	30.7	3.3
Overall Average				3.8	21.0	30.7	2.8

Table 12. Southbound Center Panel Averages for Deflection and AREA

Date	Direction	Pav Temp (°F) at 4in	No. of Tests	D0 (MILS)	D0 COV (%)	AREA (in)	AREA COV (%)
5/30/2006	SB	88	21	3.3	25.8	31.1	2.6
8/23/2001	SB	88	34	3.3	23.3	31.1	2.1
9/20/1999	SB	64	36	3.2	22.2	30.9	2.6
4/30/1997	SB		108	3.2	22.5	30.5	2.7
5/16/1995	SB	70	37	3.6	19.8	31.0	2.3
4/16/1990	SB	40	108	4.0	18.9	30.7	4.7
8/29/1989	SB	74	75	3.0	16.4	30.9	3.7
3/30/1989	SB	40	78	3.5	13.3	30.7	2.7
Overall Average				3.4	20.3	30.9	2.9

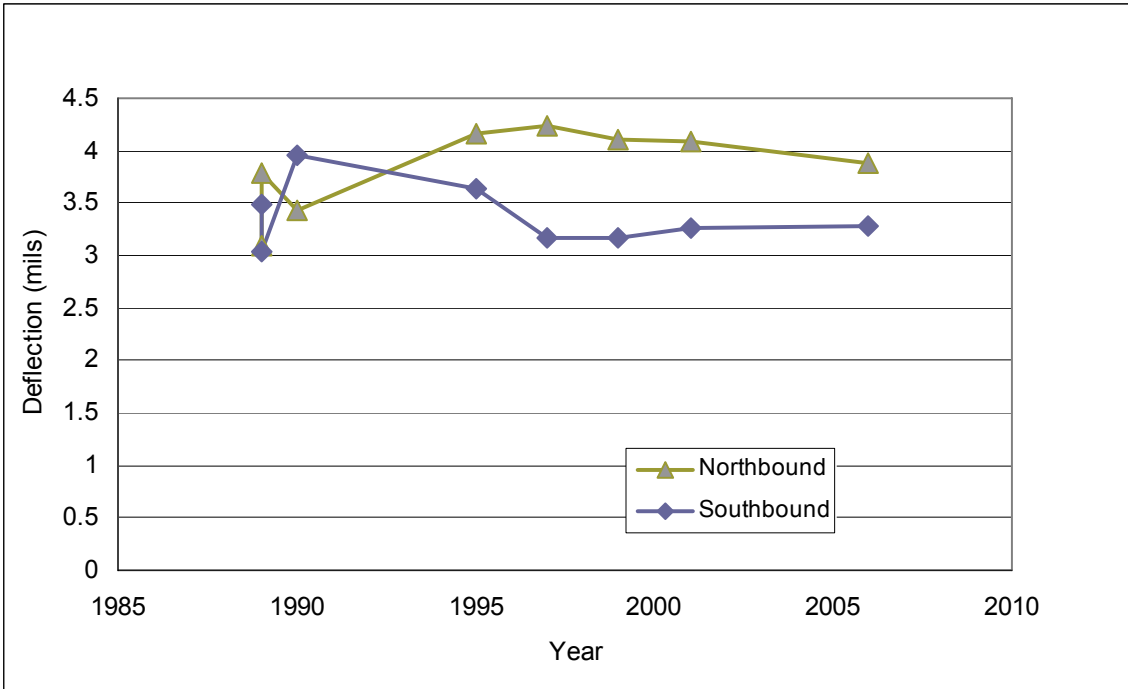


Figure 6. Average center of the driving lane deflection per direction per year

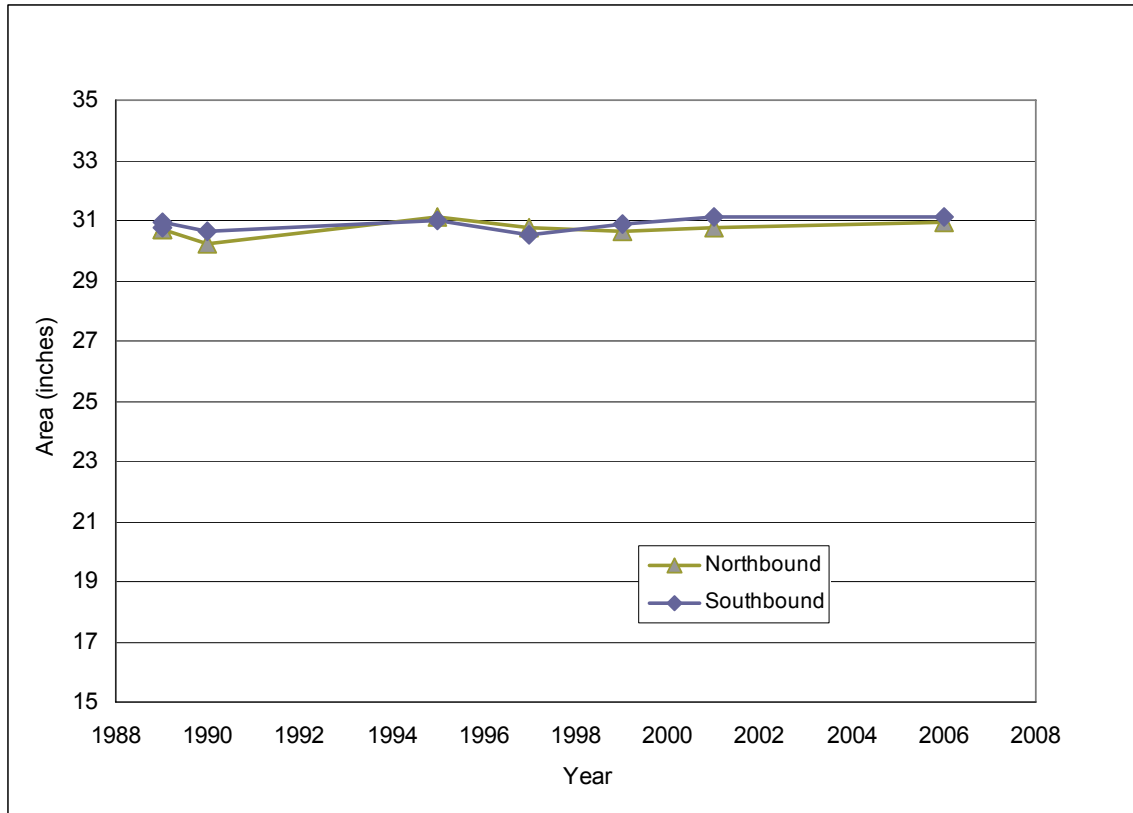


Figure 7. Average center of the driving lane AREA per direction per year

To explain some of the variability in deflection and AREA data from year to year, the data can be plotted against the pavement temperature at a 4-in depth.

Figure 8, Figure 9, Figure 10, and Figure 11 show the average center of the driving lane deflection and AREA relative to the temperature for both directions. As the temperature decreases, the general trend is for the deflection and AREA to decrease also. This is somewhat counterintuitive, since lower temperatures should open the transverse cracks and result in higher deflections. Another factor that influences the deflection is the temperature differential through the slab thickness, which was not available for these test data and therefore no conclusions can be made with respect to temperature behavior and deflection.

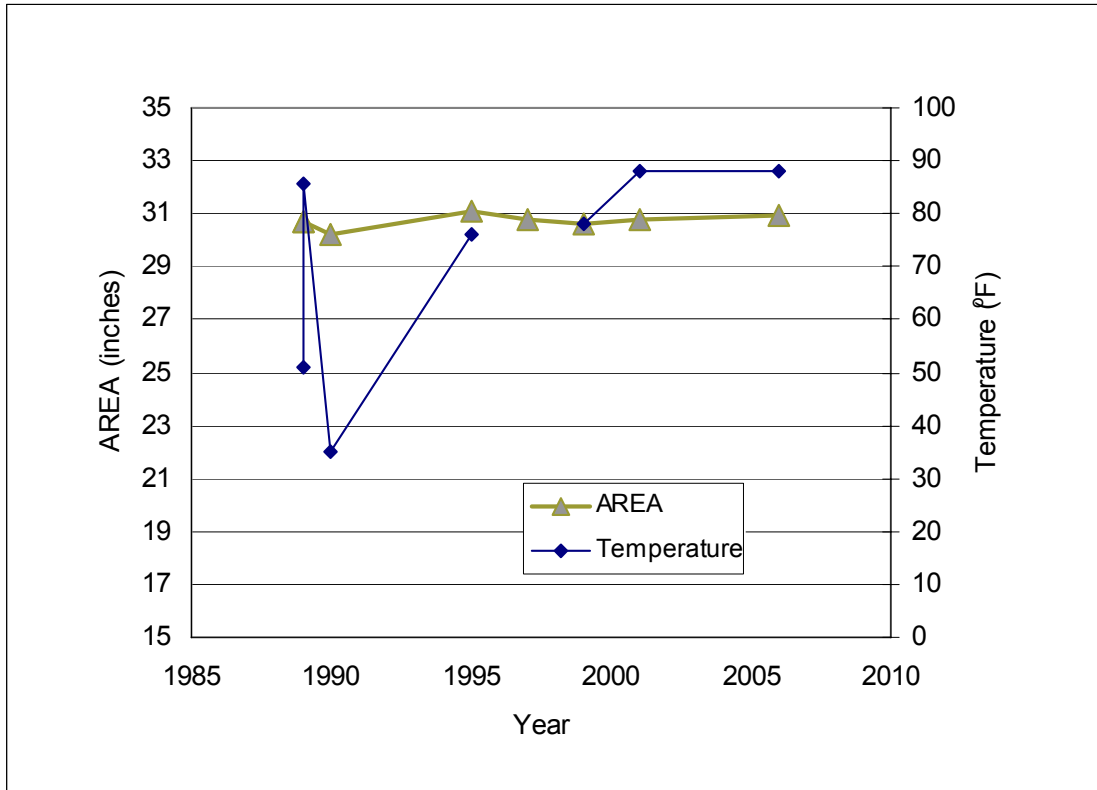


Figure 8. Average northbound center of the driving lane AREA per year

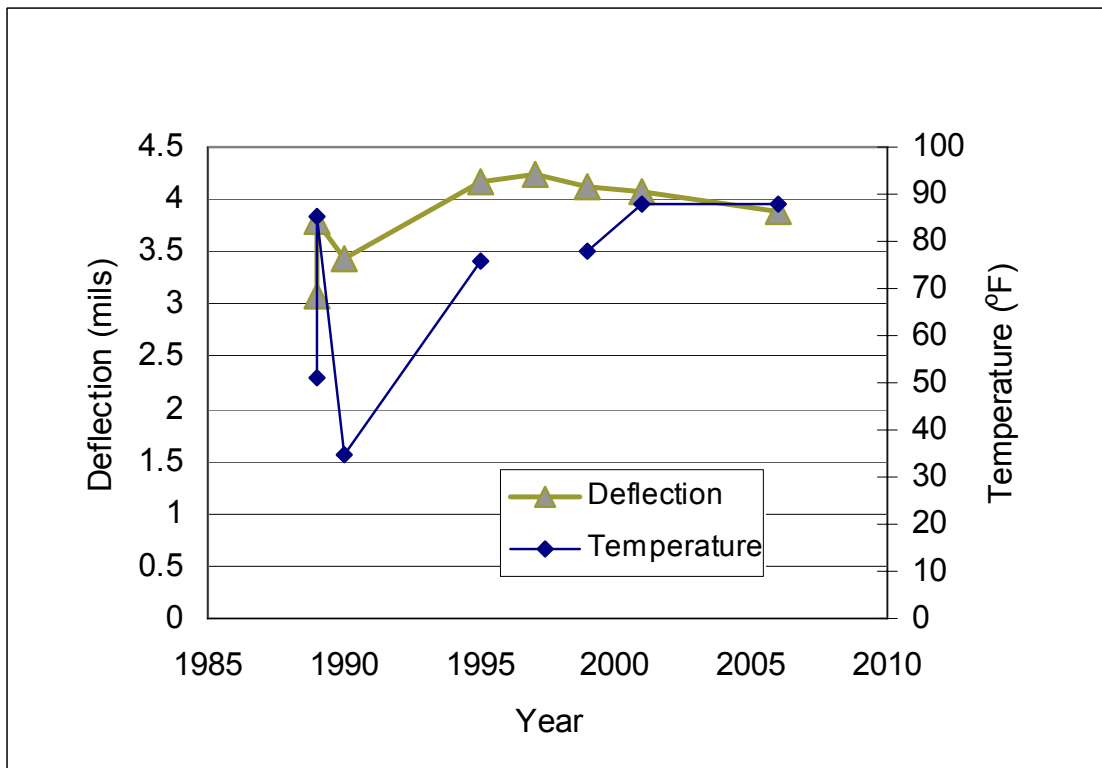


Figure 9. Average northbound center of the driving lane deflection per year

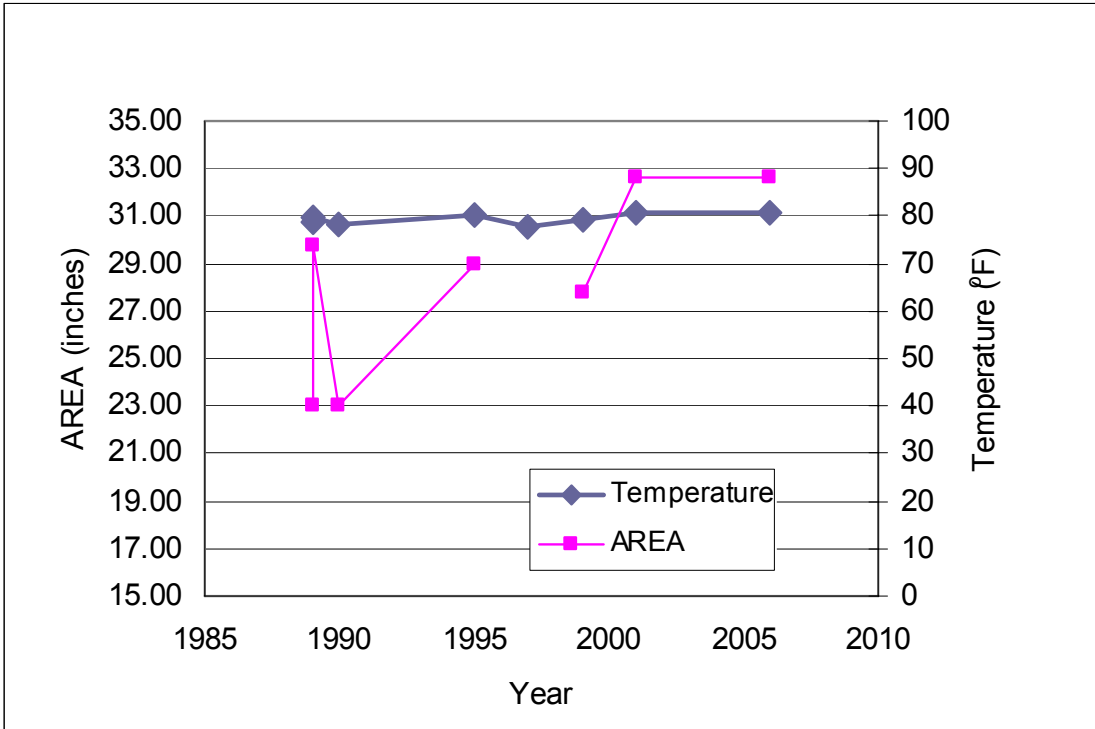


Figure 10. Average southbound center of the driving lane AREA per year

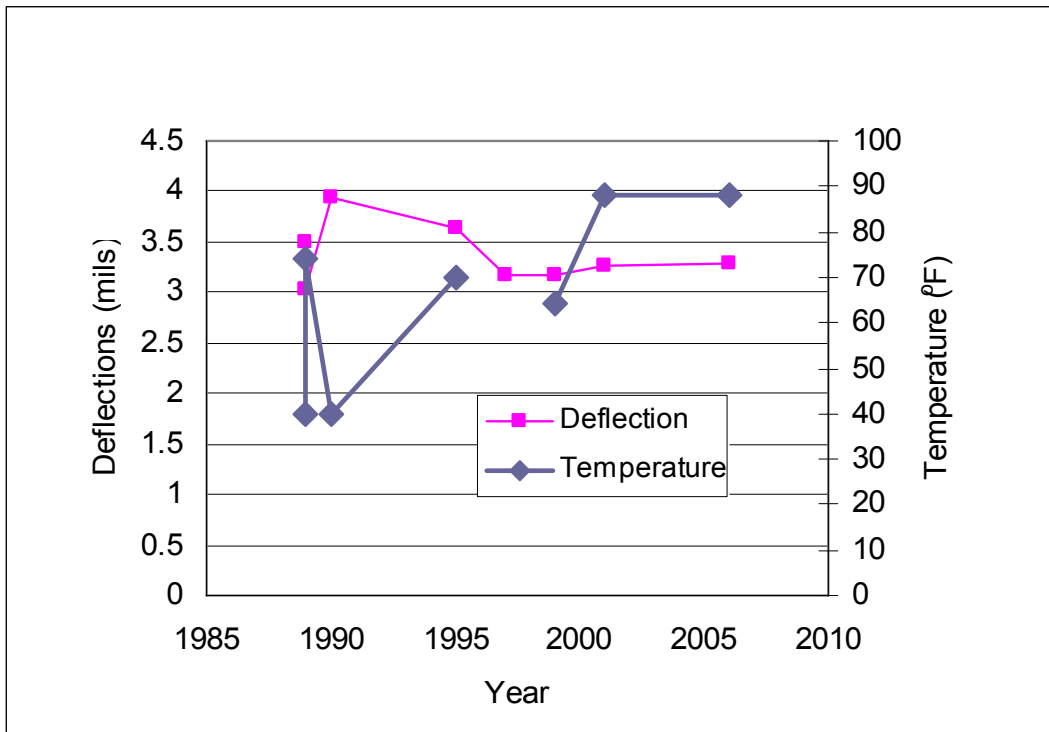


Figure 11. Average southbound center of the driving lane deflection per year

The data for the true longitudinal edge is shown in Table 13 and Table 14. As expected, the average deflection is higher at the longitudinal true edge relative to the center of the truck lane, but both are very low. The AREA terms are essentially the same for both directions and drop locations. The mean true edge deflections between the northbound and southbound are only slightly different (0.2 mils), suggesting the 24-ft versus the 27-ft cement aggregate base width has not made a difference in the CRCP structural response. Overall, the deflection data suggest that the CRCP system is still in good structural shape and has not shown any signs of measurable deterioration based on the FWD testing.

Table 13. Average Northbound True Edge Deflection and AREA

Date	Direction	Pav Temp (°F) at 4in	No. of Tests	D0 (mils)	D0 COV (%)	AREA (in)	AREA COV (%)
5/30/2006	NB	88	22	6.1	13.2	31.0	1.9
8/21/2001	NB	88	32	7.7	13.6	31.3	1.7
8/25/1999	NB	78	35	7.1	16.4	N/A	N/A
5/15/1995	NB	76	38	4.2	21.9	31.1	2.5
4/17/1990	NB	36	48	8.2	18.0	31.2	1.8
8/29/1989	NB	90	26	4.9	16.1	30.6	3.9
3/29/1989	NB	48	54	6.7	16.1	30.7	3.4
Overall Average				6.4	16.5	31.0	2.5

Table 14. Average Southbound True Edge Deflection and AREA

Date	Direction	Pav Temp (°F) at 4in	No. of Tests	D0 (mils)	D0 COV (%)	AREA (in)	AREA COV (%)
5/30/2006	SB	88	22	5.9	31.2	31.3	1.7
8/23/2001	SB	88	34	6.4	18.4	31.1	1.7
9/20/1999	SB	78	37	7.2	23.0	N/A	N/A
5/16/1995	SB	70	36	3.1	19.9	31.0	2.3
4/16/1990	SB	44	54	6.2	15.3	30.3	0.3
8/29/1989	SB	76	36	9.0	19.4	31.3	1.9
3/30/1989	SB	40	42	8.8	19.0	30.7	3.6
Overall Average				6.6	20.9	31.0	1.9

### 5.2.2 Load Transfer Efficiency (LTE)

Load transfer efficiency (LTE) was calculated by dividing the deflection on the unloaded side of the crack (D4) by the deflection on the loaded side of the crack (D0). LTE data was collected at the following three CRC slab locations: leave crack at the outer wheel path, leave crack at the striped edge, and at the true longitudinal edge. Throughout the life of this CRC pavement, only the outer wheel path location was consistently tested. The leave crack at the striped edge was tested only until 1997.

Only the leave crack and striped edge position will be presented. The true edge measurements were collected (except in 1997), but are not presented in this report. The values for LTE in the outer wheel paths are shown in Table 15, Table 16, and Figure 12. The average LTE is greater than 90 percent and the COV is less than 3 percent. This LTE value is excellent for the outer wheel path and has not shown any signs of deterioration over the past 20 years.

Table 15. Average Northbound LTE – Outer Wheel Path

Date	Direction	No. of Tests	Pav Temp (°F)	LTE (%)	COV (%)
5/30/2006	NB	42	88	91.9	2.7
8/21/2001	NB	62	88	92.0	1.5
8/25/1999	NB	69	78	92.3	1.7
4/29/1997	NB	96	N/A	91.7	1.9
5/15/1995	NB	30	76	93.2	1.3
4/1/1990	NB	102	36	92.3	3.4
8/29/1989	NB	51	90	92.3	3.3
3/29/1989	NB	102	48	92.6	2.2
Overall Average				92.3	2.2

Table 16. Average Southbound LTE – Outer Wheel Path

Date	Direction	No. of Tests	Pav Temp (°F)	LTE (%)	COV (%)
5/30/2006	SB	45	88	91.0	2.7
8/23/2001	SB	70	88	91.4	1.6
9/20/1999	SB	70	78	91.2	1.9
4/30/1997	SB	96	N/A	89.9	6.7
5/16/1995	SB	32	70	91.5	2.1
4/1/1990	SB	105	44	92.4	4.6
8/31/1989	SB	72	76	91.0	3.6
3/30/1989	SB	72	40	92.9	2.3
Overall Average				91.4	3.2

The load transfer efficiency can also be affected by temperature, similar to deflections and AREA, but as seen in Figure 12, the load transfer efficiency for these CRC sections have held constant over time.

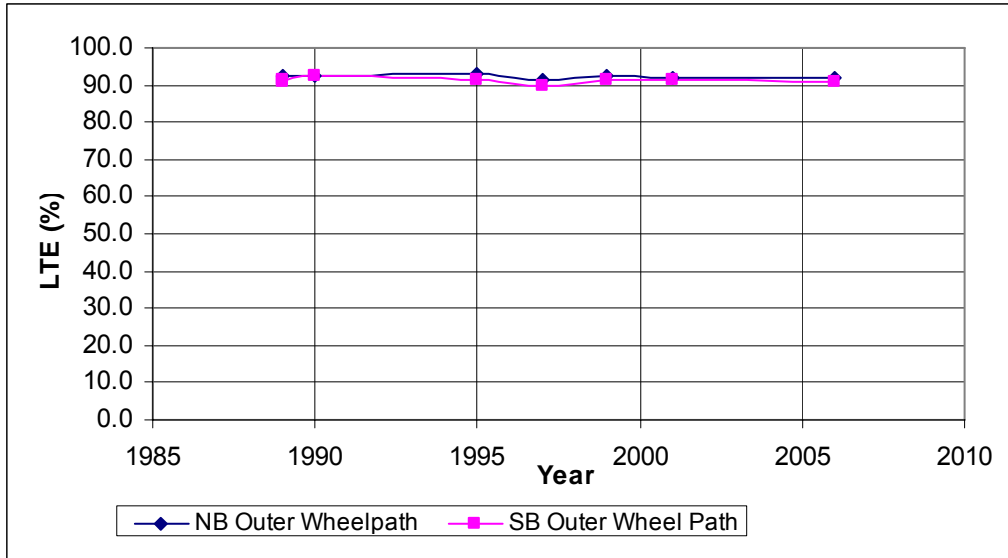


Figure 12. Load transfer efficiency at leave crack of outer wheel path

The LTE at the striped pavement edge are presented in Table 17 and Table 18. The level of deflection load transfer at this load position is high and is very similar to the outer wheel path. Overall, the LTE in both the outer wheel path and the striped edge demonstrate the transverse cracks are functioning at a high capacity, and therefore, the CRCP system is working as originally designed.

Table 17. Average Northbound LTE – Striped Edge

Date	Direction	No. of Tests	Pav Temp (°F)	LTE (%)	COV (%)
4/29/1997	NB	96	NA	92.5	1.9
5/15/1995	NB	30	76	91.4	3.9
4/17/1990	NB	105	36	93.7	3.9
8/29/1989	NB	51	90	94.3	4.3
3/29/1989	NB	96	48	92.4	4.7

Table 18. Average Southbound LTE – Striped Edge

Date	Direction	No. of Tests	Pav Temp (°F)	LTE (%)	COV (%)
4/30/1997	SB	96	NA	92.4	4.9
5/16/1995	SB	32	70	92.5	2.9
4/16/1990	SB	105	44	92.4	3.7
8/31/1989	SB	72	76	93.6	1.5
3/30/1989	SB	72	40	93.3	2.0

### 5.2.3 Subgrade Resilient Modulus

The subgrade resilient modulus ( $E_{RI}$ ) was backcalculated from the deflections at the center of the driving lane drop position. The modulus was calculated using the following equation that was developed at the University of Illinois (Thompson, 1988):

$$E_{RI} \text{ (psi)} = 25700 - 7280 * D3 + 530 * (D3)^2$$

The method uses D3, the deflection under the sensor 36 in from the center of the load, to determine the subgrade resilient modulus value. Table 19 and Table 20 show the average calculated values for each year.

Table 19. Average Northbound  $E_{RI}$ ,  $k$ -value and  $E_C$  per Year

Date	Direction	$E_{RI}$ (ksi)	$E_{RI}$ COV (%)	$k$ -value (psi/in)	$k$ -value COV (%)	$E_C$ (psi)	$E_C$ COV (%)
5/30/2006	NB	10.0	19.4	184	36.3	4.83E+06	22.2
8/21/2001	NB	9.7	23.3	198	25.7	4.80E+06	24.9
8/25/1999	NB	10.0	25.3	206	29.8	4.97E+06	41.0
4/29/1997	NB	10.0	43.5	194	43.2	4.45E+06	39.3
5/15/1995	NB	9.3	30.0	157	34.6	4.52E+06	28.2
4/17/1990	NB	11.4	14.8	249	44.4	4.34E+06	39.6
8/29/1989	NB	9.3	48.1	223	67.1	5.18E+06	70.0
3/29/1989	NB	12.7	13.3	260	47.7	5.97E+06	37.3
Overall Average		10.3		217		5.4E+06	

Table 20. Average Southbound  $E_{RI}$ ,  $k$ -value and  $E_C$  per Year

Date	Direction	$E_{RI}$ (ksi)	$E_{RI}$ COV (%)	$k$ -value (psi/in)	$k$ -value COV (%)	$E_C$ (psi)	$E_C$ COV (%)
5/30/2006	SB	11.9	23.3	214	32.6	6.41E+06	42.4
8/23/2001	SB	11.9	18.9	244	24.1	7.27E+06	40.2
9/20/1999	SB	12.4	18.6	260	41.8	6.49E+06	29.8
4/30/1997	SB	13.4	28.8	194	43.2	4.45E+06	39.3
5/16/1995	SB	12.5	15.1	208	24.9	5.93E+06	35.3
4/16/1990	SB	10.4	20.4	205	60.3	4.57E+06	57.3
8/29/1989	SB	12.5	15.2	248	65.1	6.55E+06	46.2
3/30/1989	SB	11.5	10.0	226	38.5	5.49E+06	47.0
Overall Average		12.1		225		5.9E+06	

The resilient moduli of the soil ranged for the northbound direction from 9.3 to 12.7 ksi with an overall average of 10.3. For the southbound direction, the overall average was calculated to be 12.1 with annual averages ranging from 10.4 to 13.4 ksi. A mean  $E_{RI}$  of 10 ksi or greater is considered a good soil condition. The mean  $E_{RI}$  were

slightly higher for the southbound lane. The high  $E_{RI}$  values are somewhat a result of the cement stabilized base. Overall, the  $E_{RI}$  suggests both northbound and southbound CRC pavement sections are being supported adequately by the soil/base layer.

#### 5.2.4 Modulus of Subgrade Reaction

A backcalculated modulus of subgrade reaction ( $k$ -value) is another means to evaluate the effectiveness of the in-situ support (soil and base layer) below the CRCP. These values were calculated using the 1993 AASHTO Guide method, based on the deflection of an infinite slab, which is generally not a good assumption with CRCP systems with close crack spacing. Based on the calculated AREA term, the radius of relative stiffness,  $l$ , can be obtained from the following equation:

$$l = \left[ \frac{\ln\left(\frac{36 - AREA}{1812.279}\right)}{-2.559} \right]^{4.387}$$

Using the calculated radius of relative stiffness and measured center deflection ( $D_0$ ) the  $k$ -value can be backcalculated from Westergaard's center slab deflection equation:

$$k = \left( \frac{P}{8D_0l^2} \right) \left\{ 1 + \left( \frac{1}{2\pi} \right) \left[ \ln\left(\frac{a}{2l}\right) + \gamma - 1.25 \right] \left( \frac{a}{l} \right)^2 \right\}$$

where,

$P$  = the load of the dropped weight;

$D_0$  = the normalized deflection under the standard drop load of 9 kips;

$a$  = the radius of the loaded plate (5.9 inches); and

$\gamma$  = the poisson ratio (0.15).

The calculated results are presented in Table 19 and Table 20. The average backcalculated  $k$ -value for both directions and all years is approximately 220 psi/in. The  $k$ -value is good for a typical support condition in Illinois. The southbound section has not seen any reduction in the  $k$ -value over time. The northbound section has seen a slight reduction in  $k$ -value in the past several years.

#### 5.2.5 Elastic Modulus ( $E_c$ )

The concrete's elastic modulus was determined by rearranging the radius of relative stiffness equation:

$$E_c = \frac{12(1 - \gamma^2)kl^4}{h^3}$$

where,

$\nu$  is the poisson ratio (0.15);  
 $k$  and  $l$  are values found earlier; and  
 $h$  is the thickness of the pavement, which is 10 inches.

A summary of the concrete elastic modulus values can be seen in Table 19 and Table 20. The average values for the elastic modulus are  $5.4 \times 10^6$  psi for the northbound lanes and  $5.9 \times 10^6$  psi for the southbound directions. These values are within the expected range of  $3 \times 10^6$  to  $8 \times 10^6$  psi for portland cement concrete, but are probably on the low end of a 20-year old concrete pavement. The elastic modulus values are expected to be lower due to the use of RCA. The FWD derived elastic moduli are higher than the static elastic moduli reported by Sturtevant (2007) of  $4.2 \times 10^6$  psi for northbound and  $3.9 \times 10^6$  psi for southbound, which is to be expected.

### **5.3 DISTRESS SURVEYS**

Pavement distress surveys can be used to evaluate the structural integrity and deterioration over time. Visual distress surveys were conducted in 1990, 1992, 1995, 1997, and 1999, while video van surveys were conducted in 2002 and 2007. Both the visual and video surveys were conducted for the entire project length. Based on the distress surveys, the most common distresses identified were longitudinal cracking, popouts, punchouts, and localized distress/spalling. The majority of these distresses occurred in the driving/truck lane of both the northbound and southbound directions, and almost all of the distresses appear to be related to the longitudinal crack phenomena discussed earlier.

#### **5.3.1 Longitudinal Cracking**

As discussed earlier, longitudinal cracks run parallel to the flow of traffic in both the driving and passing lanes. Based on distress surveys, longitudinal cracking has been visible since the first visual survey in 1990, and is currently very prevalent on both northbound and southbound sections. In recent visual inspections conducted by Roesler et al. (2002) and Sturtevant (2007), longitudinal cracking was present on 100 percent of the experimental CRCP section. Figure 13 shows a picture of the longitudinal cracking on the northbound lanes, while Figure 14 shows the longitudinal cracking and associated distresses in the northbound driving lane. From these photos, it is apparent that much of the subsequent distresses (popouts, localized distresses, spalls, and patches) that have developed on these CRCP sections have emanated from deteriorating longitudinal cracks.



Figure 13. Longitudinal cracking in the northbound lane



Figure 14. Longitudinal cracking and distress in the northbound driving lane

### 5.3.2 Localized Distresses, Patches, and Punchouts

Distress surveys were reviewed to show progression of the distresses in both directions. Table 21 shows a cumulative annual total for the various distresses. Until 1999, visual distresses surveys were conducted using the previous survey as a guide.

Three main types of distress were identified during these surveys: punchouts, popouts, and potholes/localized distress. Table 21 also lists the number of patches counted on the entire section.

Table 21. Total Number of Popouts, Potholes, and Punchouts Identified on Visual Distress Surveys

Year	Direction	Patches	Popouts	Potholes	Punchouts	All
1999	NB	4	0	25	2	27
1999	SB	1	3	28	4	35
1997	NB	4	0	15	2	17
1997	SB	1	3	20	4	27
1995	NB	4	0	11	0	11
1995	SB	1	3	8	1	12
1992	NB	4	0	8	0	8
1992	SB	0	0	7	1	8
1990	NB	2	0	3	0	3
1990	SB	0	0	1	0	1

For the first 15 years of service, a total of five patches were counted for both directions. In the northbound direction, two patches were present before the first survey in 1990 and therefore, no mechanism for the required early patching is known. Two more patches were identified on the 1992 survey. The 1992 survey did not identify any distresses within these locations; thus, the cause of these patches were also not known. For the southbound direction, the cause of the only patch is known. In 1990, the future patching location (5467+50 to 5467+70) was identified with a “high” severity longitudinal crack and a “medium” severity pothole. In 1992, an additional “high” severity punchout was added. In 1995, the survey shows a 15-ft-by-13.5-ft. patch in the driving lane covering the previous distress.

Given the difficulty of differentiating among the various localized distresses (popouts, potholes, or spalls) on the video surveys of 2002 and 2007, and for ease of analysis, all these distresses (see Figure 15) were classified as localized distresses. Table 22 shows the numbers of each distress identified with the video survey. Due to the level of longitudinal cracking present, it was highly unlikely that any classic punchouts had developed, and that the patches were a result of the longitudinal cracks deteriorating as a result of repeated traffic loading.



Figure 15. Localized distress in the southbound driving lane

Table 22. Total Number of Patches, Punchouts and Localized Distresses Identified on Video Distress Surveys

Year	Direction	Patches	Localized Distresses	Punchouts
2007	NB	33	17	0
2007	SB	26	1	0
2002	NB	4	0	0
2002	SB	6	8	0

Using data from both visual and video surveys, it can be seen that for the first 10 years, only a few distresses were identified, with most of those being classified as low severity with a slow deterioration rate. But, over the past 5 years as seen in Table 22, a significant rise has taken place in the number of patches and localized distresses. The localized distresses and patches almost always emanate from existing longitudinal cracks. Figure 16 and Figure 17 demonstrate that many of the distresses and patches that subsequently develop occur near previous patches.



Figure 16. Deteriorating patch in the southbound driving lane



Figure 17. Multiple CRCP patches in the southbound driving lane

### 5.3.3 Mean Crack Spacing

The mean crack spacing was calculated from the videos surveys acquired in 2002 and 2007. Three 500-ft sections were viewed on the northbound lanes, while four 500-ft sections were surveyed in the southbound direction. The mean crack spacing was determined by dividing the length of the surveyed section by the number of transverse cracks plus one counted within that section. Table 23, Table 24, and Table 25 give the mean crack spacing per direction and the overall crack spacing for a given year. The mean crack spacing in 2002 was 1.68 ft and 1.71 ft for two different locations within the same mile segment. In 2007, the mean crack spacing was 1.47 ft.

First of all, the mean spacing for separate 500-ft segments within the same mile marker for the 2002 survey data showed that the overall mean was different by only 0.03 ft, and thus, the 500-ft sample was representative of each mile's transverse cracking pattern. Second, the mean spacing has been reduced in the past 5 years from 1.71 to 1.47 ft. Figure 18 and Figure 19 demonstrate the characteristics of the transverse cracks on this CRCP with RCA. This CRCP section shows a pavement with very atypical mean crack spacing relative to CRCP with virgin coarse and fine aggregates. Typical mean crack spacings for CRCP in Illinois range from 4 to 6 ft. Table 26 shows the mean crack spacing for a CRCP on I-39 to be 4.54 ft. The extremely small crack spacing most definitively is linked to the use of recycled concrete materials exhibiting a larger drying shrinkage, coupled with a lower tensile strength and fracture resistance relative to plain concrete with virgin aggregates (Bordelon et al., 2008).

Table 23. 2002 Mean Crack Spacing and Location on I-57 (Location 1)

Segment			Mean Crack Spacing (ft)
Direction	Starting Milepost	Ending Milepost	
Northbound	165.477	165.571	1.73
	166.000	166.096	1.82
	167.095	167.190	1.66
<i>Mean Spacing North</i>			1.74
Southbound	167.867	167.772	1.63
	166.810	166.716	1.57
	165.981	165.886	1.48
	164.716	164.621	1.86
<i>Mean Spacing South</i>			1.64
<b>Overall Mean Spacing</b>			1.68

Table 24. 2002 Mean Crack Spacing and Location on I-57 (Location 2)

Segment			Mean Crack Spacing (ft)
Direction	Starting Milepost	Ending Milepost	
Northbound	165.079	165.175	1.74
	166.228	166.322	1.79
	167.000	167.095	1.97
<i>Mean Spacing North</i>			1.84
Southbound	167.564	167.47	1.76
	166.337	166.242	1.52
	165.905	165.809	1.58
	164.849	164.754	1.58
<i>Mean Spacing South</i>			1.61
<b>Overall Mean Spacing</b>			1.71

Table 25. 2007 Mean Crack Spacing and Location on I-57

Segment			Observed Crack Spacing (ft)
Direction	Starting Milepost	Ending Milepost	
Northbound	165.079	165.175	1.44
	166.228	166.324	1.64
	167.000	167.095	1.72
<i>Mean Spacing North</i>			1.60
Southbound	167.564	167.470	1.38
	166.337	166.242	1.38
	165.905	165.809	1.43
	164.849	164.754	1.27
<i>Mean Spacing South</i>			1.37
<b>Overall Mean Spacing</b>			1.47



Figure 18. Transverse cracking northbound lanes

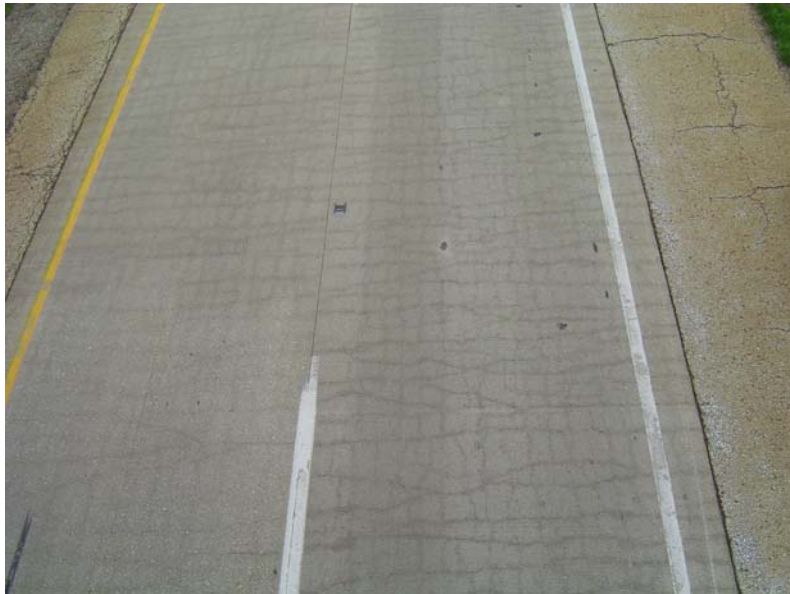


Figure 19. Transverse and longitudinal cracking northbound lanes

Table 26. Observed Crack Spacing and Location on I-39 (from Beyer and Roesler, 2008)

Direction	Segment		Observed Crack Spacing (ft)
	Starting Milepost	Ending Milepost	
Northbound	2.678	2.773	3.66
	3.354	3.449	4.78
	4.076	4.171	5.34
	5.218	5.313	5.34
Southbound	5.201	5.106	4.40
	4.609	4.514	4.82
	3.460	3.365	4.08
	2.758	2.663	3.92
Average			4.54

## 5.4 PAVEMENT STRUCTURAL PERFORMANCE

The FWD data demonstrated that the CRCP cross-section and transverse cracks are still in good structural condition for both directions. With normalized deflections less than 6 mils, this CRC pavement section should continue to carry loads, assuming the deterioration and spalling at the surface can be controlled with an overlay. The load transfer efficiency values across the transverse cracks were approximately 90 percent at the outer wheel path and the striped edge of the pavement, which signifies there is still excellent shear transfer between adjacent slab panels. The small crack spacing, and more important, the crack width have played a significant role in maintaining the high load transfer across the cracks. The average  $E_{Ri}$  is 10.3 ksi for northbound and 12.1 ksi for southbound sections. The mean  $k$ -values for both directions are approximately 220 psi/in. The measured deflections and backcalculated support conditions suggest a good pavement foundation (base and soil) for this CRCP system, and it should be able to continue to offer bearing capacity for the predicted future traffic volumes. Longitudinal cracking is the primary distress which has resulted in the appearance of other distresses and patching. It was not possible to identify structural distresses such as punchouts for this 10-in CRCP due to the extensive longitudinal cracking.

## CHAPTER 6. FUNCTIONAL EVALUATION

The functional performance of a pavement is its ability to provide a safe and comfortable ride to the roadway users. The functional performance of this RCA pavement section has been monitored by IDOT since construction. This chapter will review the collected friction, roughness, and condition rating survey data to determine the functional performance of the I-57 recycled concrete pavement section.

### 6.1 FRICTION TESTING

Friction testing was conducted approximately twice per year for the first 5 years of service, and subsequently, roughly every two years. Both treaded and smooth tire

testing were performed. The average results of these tests are highlighted in Table 27 for both northbound and southbound directions.

Table 27. Friction Testing Data

Survey Date	Northbound		Southbound	
	Treaded	Smooth	Treaded	Smooth
11/8/2007	54	42	55	47
9/16/2002	56	42	57	43
8/21/2000	58	53	59	53
9/28/1998	49	37	51	40
9/26/1996	60	47	60	48
5/20/1993	62	56	63	56
3/19/1992	62	51	64	54
6/27/1991	51	43	55	49
4/29/1991	58	49	64	58
6/13/1990	56	47	57	55
7/10/1989	51	44	55	52
4/13/1989	53	49	58	54
10/13/1988	50	44	55	52
7/13/1988	47	41	58	51
4/19/1988	55	49	58	53
10/21/1987	54	52	60	63
8/3/1987	56	49	N/A	N/A
4/7/1987	51	52	N/A	N/A

The southbound section was not completed until late in 1987; thus no data exists for the spring of that year. The treaded tire results show that the friction number has varied little over the 20-year life of the pavement, which can be seen in Figure 20. The smooth tire data show a 10-point decrease on the northbound and an approximately 15-point decrease on the southbound after 20 years. IDOT considers friction values above 35 for the treaded tire and 25 for the smooth tire tests to be good and to not be a factor in contributing to wet weather accidents. Thus, the northbound and southbound lanes meet the criteria for adequate friction values.



Figure 20. Changes in treaded and smooth friction data over time

## 6.2 INTERNATIONAL ROUGHNESS INDEX

The International Roughness Index (IRI) is the most widely used standard to quantify the roughness or smoothness of a pavement. It summarizes the longitudinal surface profile deviation from a perfectly smooth condition. Profiles of this RCA pavement section have been gathered annually since 1990, typically in the summer months such as June, July, and August; except for 1999 and 2001, when the tests were conducted, respectively, in April and March,. Tests performed in 1990, 1991, and 1992 used the Illinois Road profiler, modeled after the South Dakota profiler. Tests taken after that date have used data collection vehicles (DCVs) equipped with video inspection equipment. All IRI values are reported in units of in per mile. The higher the IRI values, the rougher the pavement section.

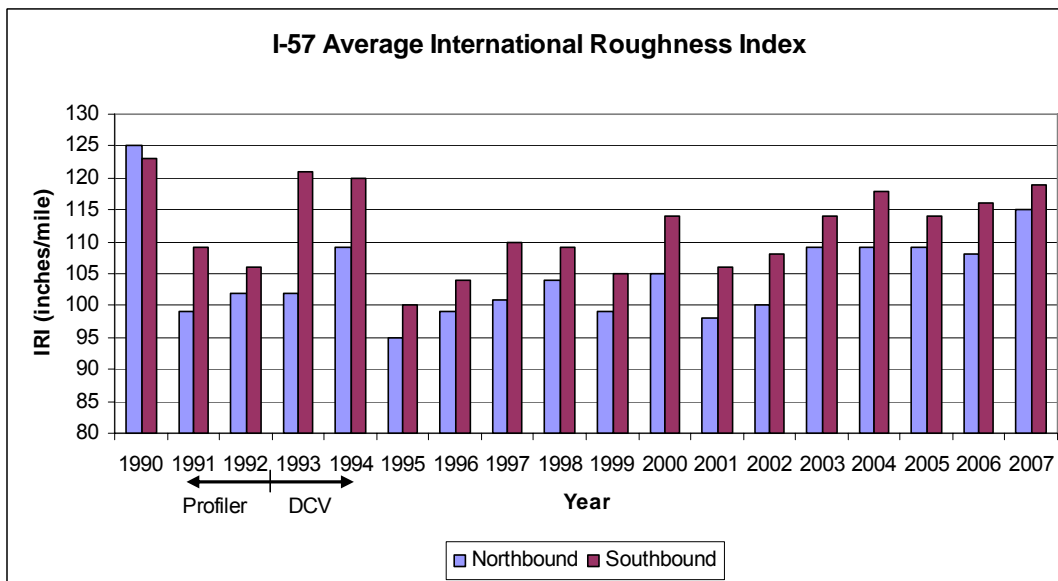


Figure 21. I-57 average IRI per year per direction

Figure 21 plots the average IRI values for I-57 with northbound and southbound directions shown separately. The data shows IRI values from 95 to 125 in per mile for northbound and 100 to 122 in per mile for southbound. A change in testing devices occurred in 1993; thus, the possible increase in IRI values for 1993 and 1994 could be attributed to the new equipment. A typical new concrete pavement has an IRI of around 60 in per mile. The initial IRI values for these sections were high but have not significantly increased over the past 15 years.

IDOT does not have thresholds for IRI, but a rule of thumb is to consider a value of approximately 100 in per mile and below as a “good” pavement, under 190 in per mile as a “fair” pavement, and a value of 225 in per mile and above as a “rough” pavement. The new M-EPDG software (ARA 2007) recommends a terminal IRI at the end of the pavement design life of 160 in per mile. Based on these IRI metrics, both sections have a fair-to-good ride quality.

### 6.3 CONDITION RATING SURVEY (CRS)

IDOT has performed condition rating surveys every two years for these sections. The CRS values are used to evaluate a pavement’s changing condition with time and how it relates to the condition of the pavements in the network for maintenance or rehabilitation planning. CRS values range from 1.0 to 9.0, with 9.0 being the value given to new construction and 1.0 representing total pavement failure. With the CRS, a large variance exists, depending on the engineer who performs the test. Table 28 and Figure 22 show a time series summary of the CRS values for the I-57 CRC pavement with RCA. The CRS values indicate a pavement that has been in good condition over its service life. Figure 22 shows a pavement that was in good condition for the first 12 to 15 years, but has shown a decline over the last 2 to 4 years due to the deteriorating longitudinal cracks.

Table 28. Summary of CRS Data

Date	CRS
Nov-06	6.0
Oct-04	6.9
Oct-02	7.0
Oct-98	7.6
Sep-96	7.7
Oct-94	8.1
Oct-92	8.5
Dec-90	8.8
Sep-88	8.8
Aug-86	9.0

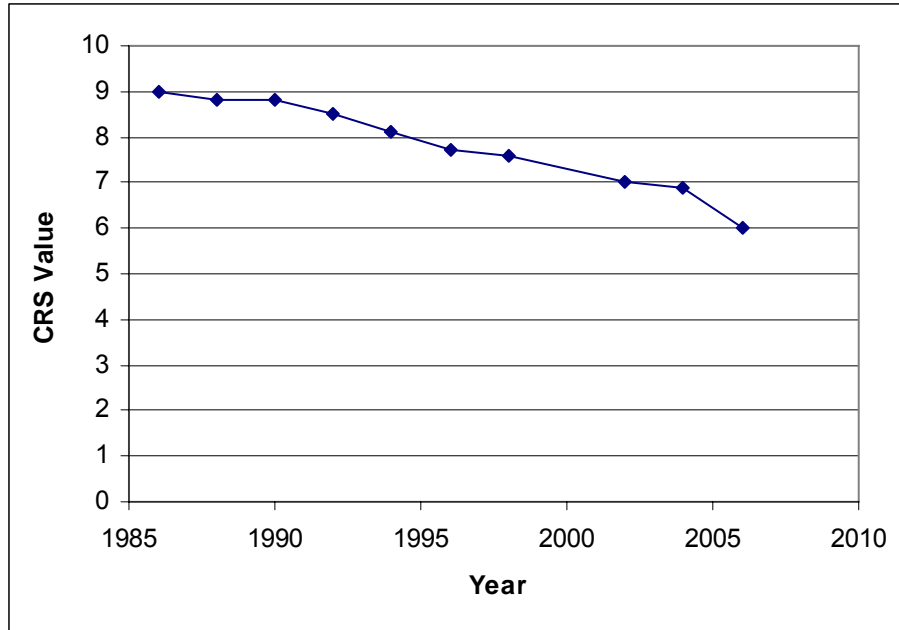


Figure 22. CRS values of pavement life

#### 6.4 SUMMARY OF I-57 FUNCTIONAL PERFORMANCE

The friction data reflects a pavement that is safe for stopping adequately. The treaded friction numbers have been consistently measured in the 50's throughout the life of the pavement. The smooth tire friction numbers have shown a steady decline, but still with values in the 40's. Both the measured treaded and smooth values exceed the IDOT thresholds of 35 and 25, specified for treaded and smooth tire friction testing. The IRI data indicate a pavement with an estimated fair-to-good ride quality, with IRI values ranging from 95 to 125 for both directions. In addition, a steady increase in IRI values has been noticed. The CRS values show a pavement with slow deterioration over the first 12 to 15 years, but recently, with a larger decrease in values, prompting the need to consider rehabilitation soon.

### CHAPTER 7. PERFORMANCE OF COMPARABLE CRCP IN ILLINOIS

In 2000, the latest round of Illinois pavement longevity studies was conducted by Gharaibeh and Darter (2002). This research study analyzed failure rates based on age and traffic loading (ESALs) for various pavement types and thicknesses, and also provided models for predicting the probability of survival of the different pavement types. Pavement failure in the 2002 study was defined as when an AC overlay was placed on the original CRCP. For 10-in CRCP, only the northern region pavement data without D-cracking was useful for comparative analysis. Gharaibeh and Darter reported that 25 percent of the 10-in CRCPs failed at 19.5 years, with an average of 31 million ESALs, and 50 percent of the pavements failed at 23 years with 40 to 90 million ESALs. The performance of the I-57 CRCP with RCA is close to the mean performance of other 10-in

CRCP around the state of Illinois in terms of age. The estimated number of ESALs for the I-57 RCA section has been 29 million, which is considerably lower than the ESALs experienced in northern Illinois, which includes the Chicago area. For 9-in CRCPs without D-cracking located in southern Illinois, the mean failure has been at 27 years and 23 million ESALs. One consideration in the Gharaibeh and Darter study was that several steel contents and base types (BAM and CAM) were used, and CRCP failure was only defined in terms of service life, not in terms of the number of punchouts.

## **CHAPTER 8. RECOMMENDATIONS FOR FUTURE RECYCLED CONCRETE PAVEMENTS IN ILLINOIS**

Based on the performance of the I-57 CRCP containing RCA, the design and material selection of future RCA pavements should continue in Illinois. When deciding to construct with RCA, a thorough evaluation of the constituent materials must be conducted relative to virgin concrete to avoid premature cracking that could be associated with D-cracking, ASR, steel corrosion, and excessive drying shrinkage. IDOT's current freeze-thaw durability test appears to have been verified for the I-57 RCA project. IDOT's sodium sulfate test for soundness initially rejected the RCA material, but has proven to be a poor correlation to its actual field performance. Although ASR has traditionally not been an issue for carbonate coarse aggregate sources in Illinois, the sand fraction needs to be checked with the proposed cementitious materials. If recycled concrete is going to be used in CRCP, the chloride content of the crushed concrete should be tested to make sure excessive free chlorides do not exist that may promote premature steel corrosion.

Due to the higher old mortar fraction on the RCA, the new concrete containing RCA has a lower elastic modulus and higher drying shrinkage potential. To overcome any potential for premature cracking from drying shrinkage, moist curing for a period of time after construction could be employed to allow the concrete to gain strength prior to drying. Another option is to use the recycled concrete in the bottom layer of a two-lift paving operation, which has been successfully completed in Europe for many years (Tompkins et al., 2009). By placing the RCA concrete in the bottom lift, drying shrinkage will be minimized, since there is little possibility for external drying; i.e., loss of capillary moisture. Although the tensile strength of RCA concrete has been known to be slightly less, recent testing has demonstrated that the fracture energy of RCA concrete is significantly less than virgin coarse aggregate concrete (Bordelon et al., 2008). The significance of lower fracture energy is that cracks propagate more easily once they have initiated; e.g., from early-age drying shrinkage cracks. The fracture properties of concrete containing RCA have been shown to equal or exceed virgin aggregate concrete when blending the RCA with virgin coarse aggregate; e.g., 50 percent by volume, or when dosing with a lower volume fraction of structural fibers (Bordelon et al., 2008).

## **CHAPTER 9. CONCLUSIONS**

This research study was conducted to evaluate the 20-year performance of the I-57 CRCP demonstration project containing recycled concrete aggregates (RCA). The pavement section consisted of a 10-in CRCP over an in-place, 7-in cement stabilized aggregate subbase layer with an asphalt shoulder. This section also has one of IDOT's few 13.5-ft extended lanes in both the driving and passing lanes. This experimental

pavement section was structurally designed for a 20-year life. The longitudinal reinforcement without epoxy coating was set at 0.7 percent and accommodated with #7 bars placed at 8-5/8 inch centers. The reinforcing in the longitudinal contraction joint was #5 bars, 2.5 ft in length at 2.5-ft centers. Standard pavement construction methods were used throughout the project, with the longitudinal reinforcement being placed using the tube feeding method. The northbound and southbound lanes were constructed in 1986 and 1987, respectively. Through 2008, it is estimated this pavement will have carried 29.1 million ESALs.

Structural and functional testing has been conducted throughout the life of the pavement. Structurally, the data show that the CRCP, cement-stabilized aggregate subbase, and the subgrade have been performing well. The pavement surface deflections under a 9-kip FWD load were found to be below  $6 \times 10^{-3}$  in, the mean AREA term was approximately 30 in, load transfer efficiencies were greater than 90 percent, and the mean concrete elastic modulus was around  $5.6 \times 10^6$  psi. The edge deflections between the northbound and southbound are only slightly different ( $0.2 \times 10^{-3}$ ), suggesting that the 24-ft. versus the 27-ft. cement aggregate base width has not made a difference in the structural response of the CRCP. The subgrade had a backcalculated subgrade resilient modulus range above 10 ksi and a modulus of subgrade reaction (*k*-value) above 200 psi/in. Functionally, the data shows pavement with good skid resistance with treaded values in the mid-50's and smooth friction values in the high 40's to low 50's range. The IRI values ranging from 100 to 120 in per mile indicate a pavement with a fair-to-good ride quality. Last, condition rating surveys show a pavement condition deteriorating in recent years, with a large number of patches occurring in certain areas. The section will be in need of a significant rehabilitation in the coming years due to the continuing longitudinal crack deterioration.

The use of RCA has not significantly hindered the performance of this extended-width CRCP section. Overall, the mean failure age of 10-in CRCP sections has been 23 years in Illinois. The main distress (longitudinal cracking) on the section is related to the initial construction, which used tube feeding of the longitudinal steel. This distress has been seen on other CRCP sections in the state, and thus is not unique to the use of RCA. The patching completed to date on this section is primarily related to the deterioration of the longitudinal cracks, and thus the structural performance in terms of punchouts has been excellent. Based on the performance of the I-57 CRCP section, crushed concrete as an aggregate in the surface concrete layer should be considered for future concrete pavement projects as long as the recycled concrete material passes the freeze-thaw requirements, accommodations are made for greater drying shrinkage and slightly lower tensile strength, and the concrete is checked for the possibility of ASR.

## CHAPTER 10. REFERENCES

American Concrete Institute Committee 201. (1994). *Guide to Durable Concrete, Chapter IV – Corrosion of Steel and other Materials Embedded in Concrete*, Manual of Concrete Practice, Part 1, Detroit, MI: American Concrete Institute,.

ARA, Inc. (2007). *Interim Mechanistic-Empirical Pavement Design Guide Manual of Practice*. Final Draft. National Cooperative Highway Research Program Project 1-37A. Transportation Research Board, Washington, D.C.

Bentur, A., Diamond, S., and Berke, N.S. (1997). *Steel Corrosion in Concrete: Fundamentals and Civil Engineering Practice*. London, UK: E & FN SPON, Taylor & Francis Group,.

Beyer, M. and Roesler, J.R. (2009). *Mechanistic-Empirical Design Concepts for Continuously Reinforced Concrete Pavements in Illinois*. Final Report, Illinois Center for Transportation, University of Illinois, Champaign-Urbana, 80 pp.

Bordelon, A., Cervantes, V. and Roesler, J. Fracture Properties of Concrete Containing Recycled Concrete Aggregate, *Magazine of Concrete Research* (submitted for publication).

Cuttell, G. D., Synder, M. B., Vandenbossche, J. M., and Wade, M. J.. (1997 ). Performance of Rigid Pavements Containing Recycled Concrete Aggregates. *Transportation Research Record 1574*, TRB, National Research Council, Washington, DC, pp 89-98,.

Embacher, R.A. (1999). Mitigation of Recurrent D-Cracking in Portland Cement Concrete Comprising Recycled Concrete Aggregate. In D..J. Janssen, M.J. Setzer, M.B. Snyder (Eds ), *Frost Damage in Concrete*, Minneapolis, MN: RILEM.

Federal Highway Administration. (2004 September). *Transportation Applications of Recycled Concrete Aggregate*, U.S. Department of Transportation, Washington, D.C., 47 pp.

Fergus, J. S. (1980). *The Effect of Mix Design on the Design of Pavement Structures When Utilizing Recycled Portland Cement Concrete as Aggregate*. PhD thesis. Department of Civil Engineering, Michigan State University, East Lansing, MI.

Gharaibeh, N. and Darter, M. I. (2002). *Longevity of Highway Pavements in Illinois – 2000 Update* (UILU-ENG-2002-2011). Illinois Cooperative Highway Research Report No. IHR-R24 for Illinois Department of Transportation, University of Illinois, Urbana-Champaign, IL.

Illinois Department of Transportation. (2002). *Bureau of Design and Environment Manual*. Bureau of Design and Environment, IDOT, Springfield, IL,.

IDOT District 7. (1998, Spring). *Coring Observations of Experimental Section of Interstate 57 North of Effingham*, Illinois Department of Transportation, Springfield, IL,.

- Richard Barksdale (ed.) (1991). *Aggregate Handbook* , Washington, D.C.: National Stone Association,.
- Peterson, K. (2008). *Report on Petrographic Examination of Cores from Concrete Pavement*, Michigan Technological University, Houghton, MI,
- Roesler, J. and Ulreich, G. (2002, September). *Investigation of Longitudinal Cracking Distress on Continuously Reinforced Concrete Pavements in Illinois*. Report for Illinois Department of Transportation, University of Illinois, Urbana-Champaign, IL.
- Roesler, J.R., Popovics, J.S., and Ranchoero, J.L. (2003, June). *Laboratory Investigation of Longitudinal Cracking on I-57 Continuously Reinforced Concrete Slab*.. Report for Illinois Department of Transportation. University of Illinois, Urbana-Champaign, IL. .
- Roesler, J.R., Popovics, J.S., Ranchoero, J.L., Mueller, M., and Lippert, D. (2005). Longitudinal Cracking Distress on Continuously Reinforced Concrete Pavements in Illinois, *ASCE Journal of Performance of Constructed Facilities*, 19 (4), pp. 331-338.
- Schutzbach, A. M. (1993, February ) Recycling Old PCC Pavement – Performance Evaluation of FAI57 Inlays.. *Physical Research No. 113*. Illinois Department of Transportation, Springfield, IL. .
- Sturtevant, J. R. (2007). *Performance of Rigid Pavement Containing Recycled Concrete Aggregate*.. MS thesis. University of New Hampshire, Durham, NH,.
- Snyder, M. B., Vandenbossche, J. M. , Smith, K. D., and Wade, M. (1994, August ). *Physical and Mechanical Properties of Recycled PCC Aggregate Concrete – Interim Report-Task A*.. Federal Highway Administration, Washington, D.C. .
- Thompson, M. ILLI-PAVE Based NDT Analysis Procedures. Proceedings, *ASTM International Symposium on Non-Destructive Testing of Pavement Structures*, ASTM Annual Meeting, Baltimore, MD, .1998, ASTM, West Conshohocken, PA.
- Tompkins, D., Khazanovich, L., Darter, M. , and Fleischer, W.. Design and Construction of Sustainable Pavements: Austrian and German Two-Layer Concrete Pavements. *Transportation Research Record: Journal of the Transportation Research Board* Transportation Research Board of the National Academies, Washington, D.C.(submitted for publication)
- Vandenbossche, Julie M. And Mark B. Synder. (1993 , October and 1994 , March ) *Uses of Recycled Portland Cement Concrete: State-of-the-Art*. Final Report , Volumes I, II and III, Lansing, MI: Michigan Concrete Pavement Association. .
- Van Matre, F. R. and Schutzbach, A. M.. Illinois' Experience with a Recycled Concrete Inlay. *Proceedings: Fourth International Conference on Concrete Pavement Design and Rehabilitation*. Purdue University, West Lafayette, IN, April 18-20, 1989, pp. 625-639.
- Vollmer, D. B. (2002, May 10). *Petrographic Examination and Chloride Analysis of Concrete Cores From Pavements, Illinois*. (CTL Project No. 151812). Skokie, IL: Construction Technology Laboratories, Inc....

Wade, M. J., Cuttell, G. D. , Vandebossche, J. M., Smith,K.D., Snyder, M.B., and Yu, H. T. (1995). *Performance of Concrete Pavements Containing Recycled Concrete Aggregate* (Report No. DTFH61-93-C-00133 - Task B ) Interim Report. Federal Highway Administration, Washington, D.C..

## APPENDIX A

# APPENDIX A. REPORT ON PETROGRAPHIC EXAMINATION OF CORES FROM CONCRETE PAVEMENT

Prepared by:

Karl Peterson  
Michigan Tech Transportation Institute  
Michigan Technological University  
1400 Townsend Drive  
Houghton, MI 49931

Prepared for:

Jeffery Roesler  
Department of Civil and Environmental Engineering  
University of Illinois Urbana-Champaign  
205 North Mathews Ave.  
Urbana, IL 61801-2352

August 28, 2008

## **Report on Petrographic Examination of Cores from Concrete Pavement**

### ***A.1 Results of Macroscopic Examination:***

Four full-depth 10½” to 11” cores were received, as shown in Figures A.1 and A.2; two cores from a north-bound lane of Interstate 57, and two cores from a south-bound lane of Interstate 57. All of the cores exhibited prominent surface cracks running perpendicular to the tining marks, as illustrated in the bottom halves of Figures A.1 and A.2. Relatively fewer cracks running along the troughs of the tining marks were also observed. Cores NB-4 and SB-4 both intersected steel reinforcement at depths of 5” and 5½” respectively. The steel reinforcement in both cases was in good condition and without corrosion. The coarse aggregate in all of the cores was a recycled concrete aggregate with a 1” top size. The coarse aggregate in the original recycled concrete was from a quarried carbonate source. A considerable proportion of the original recycled concrete mortar was also present in the recycled concrete coarse aggregate.

The cores labeled NB-2 and SB-2 were each cut in half at approximately mid-depth. Slabs were subsequently cut and polished to represent both the bottom and top halves in cross-section for each core as shown in Figures A.3 through A.6. Two sets of slabs were polished from each core. The first set of slabs were scanned as-polished, after staining with a solution of phenolphthalein, (to check carbonation depth) and after a black and white treatment to enhance the visibility of cracks and air voids, (as shown in Figures A.3 and A.5). The scanned images from the black and white treated slabs were later used to perform automated air-void analyses. The second set of slabs were scanned as-polished and after staining with a solution of sodium cobaltinitrite, (to check for potassium-bearing alkali silica reaction products).

Detailed scanned images from selected slabs are included in Figures A.7 through A.9. Figure A.7 illustrates the typical appearance of the surface cracks in cross section, as indicated by black arrows. The cracks propagate through the hardened paste to depths of approximately 1”. Figure A.8 illustrates the depth of carbonation, approximately ¼”. Figure A.9 shows that the sodium cobaltinitrite stain was picked up strongly by some of the fine aggregate particles. The yellow stain was also picked up faintly by the carbonate fraction of the recycled concrete coarse aggregate particles, as well as along a ¼” band just below the pavement surface.

### ***A.2 Results of Microscopic Examination:***

The polished slabs were examined with a zoom stereo microscope. Figure A.10 shows a recycled concrete coarse aggregate particle. The coarse aggregate particle shown in Figure A.10 contains a considerable proportion of adhered mortar. For purposes of calculating air void parameters, the adhered cement paste fraction of the recycled concrete coarse aggregate was included as part of the cement paste fraction of the new concrete. The end of this report contains the results of the automated air-void analyses. A

single lump of asphalt was also observed in a slab from the top-half of core NB-2 as shown in Figure A.11, (the same lump is also visible in Figure A.3).

Figures A.12 through A.14 show examples of alkali-silica reaction in fine aggregate particles both before and after application of the sodium cobaltinitrite stain. In Figures A.12 and A.13, blobs of alkali-silica reaction product are clearly visible adjacent to the aggregate particles. In Figures A.13 and A.14, faint cracks can be observed within the reactive aggregate particles.

Figures A.15 through A.17 show examples of the carbonate fraction of the recycled coarse aggregate particles both before and after application of the sodium cobaltinitrite stain. Many of the carbonate particles exhibited a darkened discoloration near the contact with the surrounding cement paste matrix. Some of the carbonate particles picked up the stain directly, but in many cases, the cement paste immediately surrounding the carbonate particles was stained yellow. The large recycled concrete coarse aggregate particle shown in the center of Figure A.17 was included to illustrate paint adhered to the original concrete surface. Figure A.18 shows alkali-silica reaction product filling a large entrapped air void adjacent to the carbonate fraction of a recycled concrete aggregate particle, as well as alkali-silica reaction product filling a small air void adjacent to a fine aggregate siltstone particle.

### **A.3 Conclusions**

The cracks observed at the pavement surface likely originated from drying shrinkage. The alkali-silica reactivity observed in the coarse aggregate particles does not appear to have resulted in expansion, as no related cracking was observed. Cracking (only two instances) was observed in reactive fine aggregate particles, but the cracks were limited to the particles themselves, without any cracking of the surrounding cement paste matrix. For the most part, reactive fine aggregate particles did not exhibit any signs of cracking or expansion. Since alkalis in concrete tend to be mobile, there is often a potassium-gradient at the pavement surface, and it is normal for the sodium-cobaltinitrite stain to be picked-up just below the pavement surface. The entrained air parameters appeared sufficient for freeze-thaw durability, with spacing factor values in the range of 0.106 – 0.143 mm, and specific surface values in the range of 25.6 to 32.5 mm<sup>-1</sup>. The carbonation depth of 1/4" is deeper than is generally expected for a concrete pavement. Carbonation depths on the order of 1/10" are more common. The deep carbonation suggests a hardened cement paste that might be slightly more permeable than would generally be expected for concrete pavement.



I-57 NB-2

I-57 NB-4

Figure A.1: 6" diameter cores I-57 NB-2 and I-57 NB-4 as-received.



I-57 SB-2

I-57 SB-4

Figure A.2: 6" diameter cores I-57 SB-2 and I-57 SB-4 as-received.

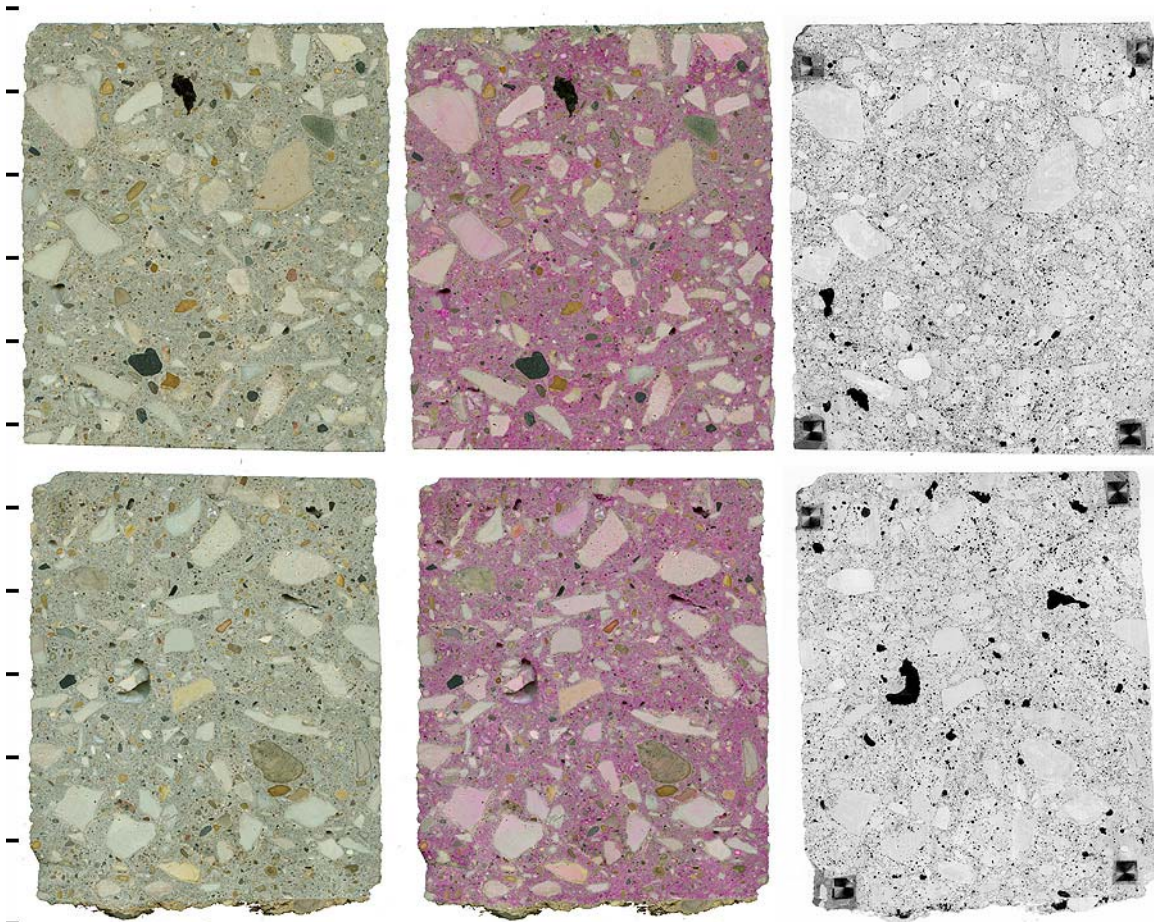


Figure A.3: First set of slabs from core NB-2, from left to right: as polished, phenolphthalein stained, and after treatment to enhance visibility of cracks and air voids, tic marks along left-hand side spaced at 1" intervals.

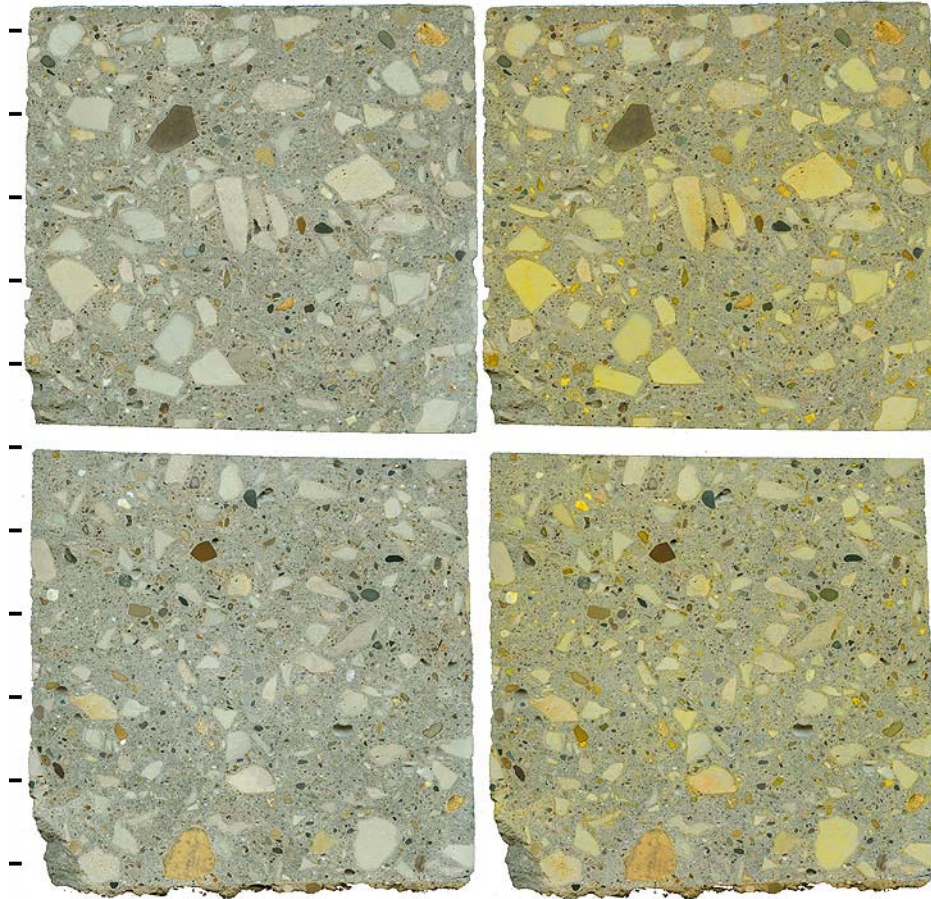


Figure A.4: Second set of slabs from core NB-2, from left to right: as polished, and sodium cobaltinitrite stained, tic marks along left-hand side spaced at 1" intervals.

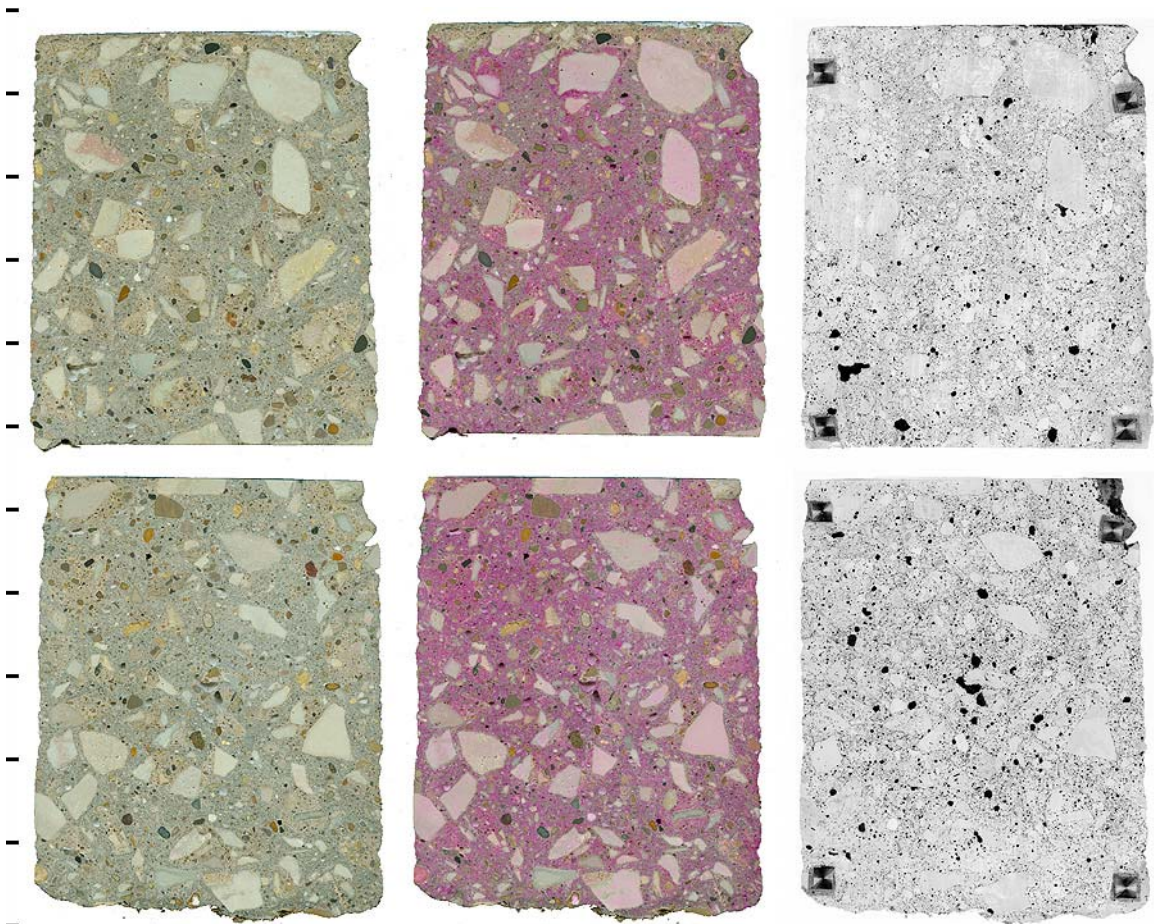


Figure A.5: First set of slabs from core SB-2, from left to right: as polished, phenolphthalein stained, and after treatment to enhance visibility of cracks and air voids, tic marks along left-hand side spaced at 1" intervals.

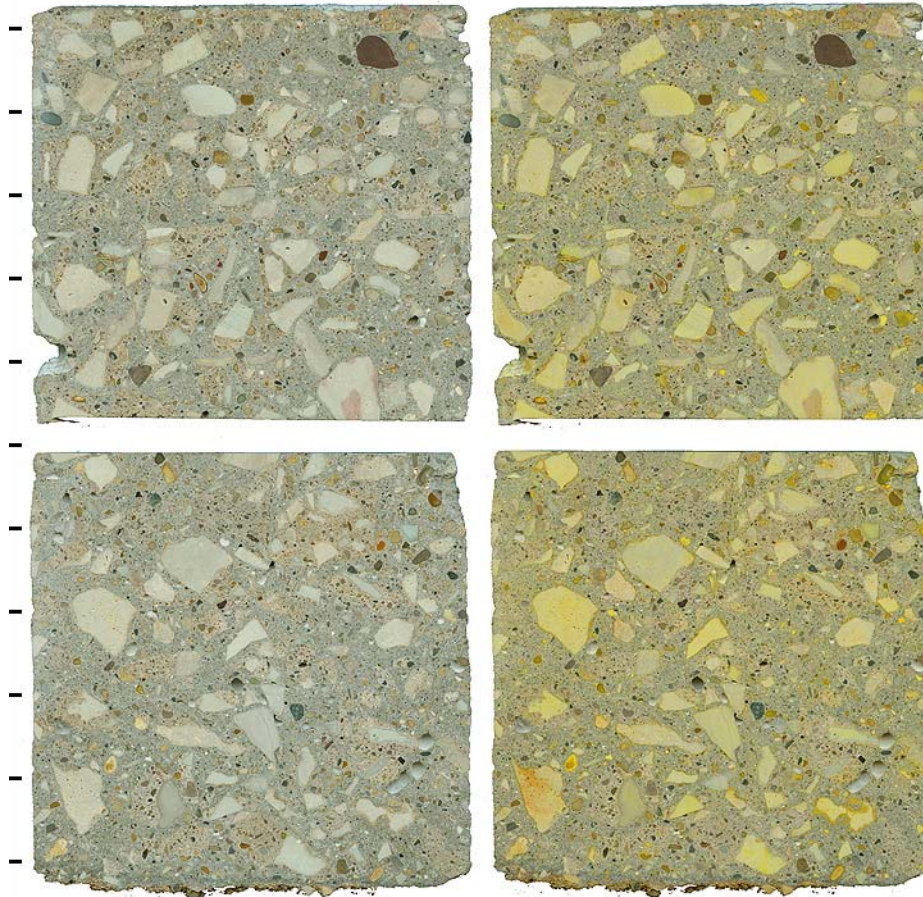


Figure A.6: Second set of slabs from core SB-2, from left to right: as polished, and sodium cobaltinitrite stained, tic marks along left-hand side spaced at 1" intervals.

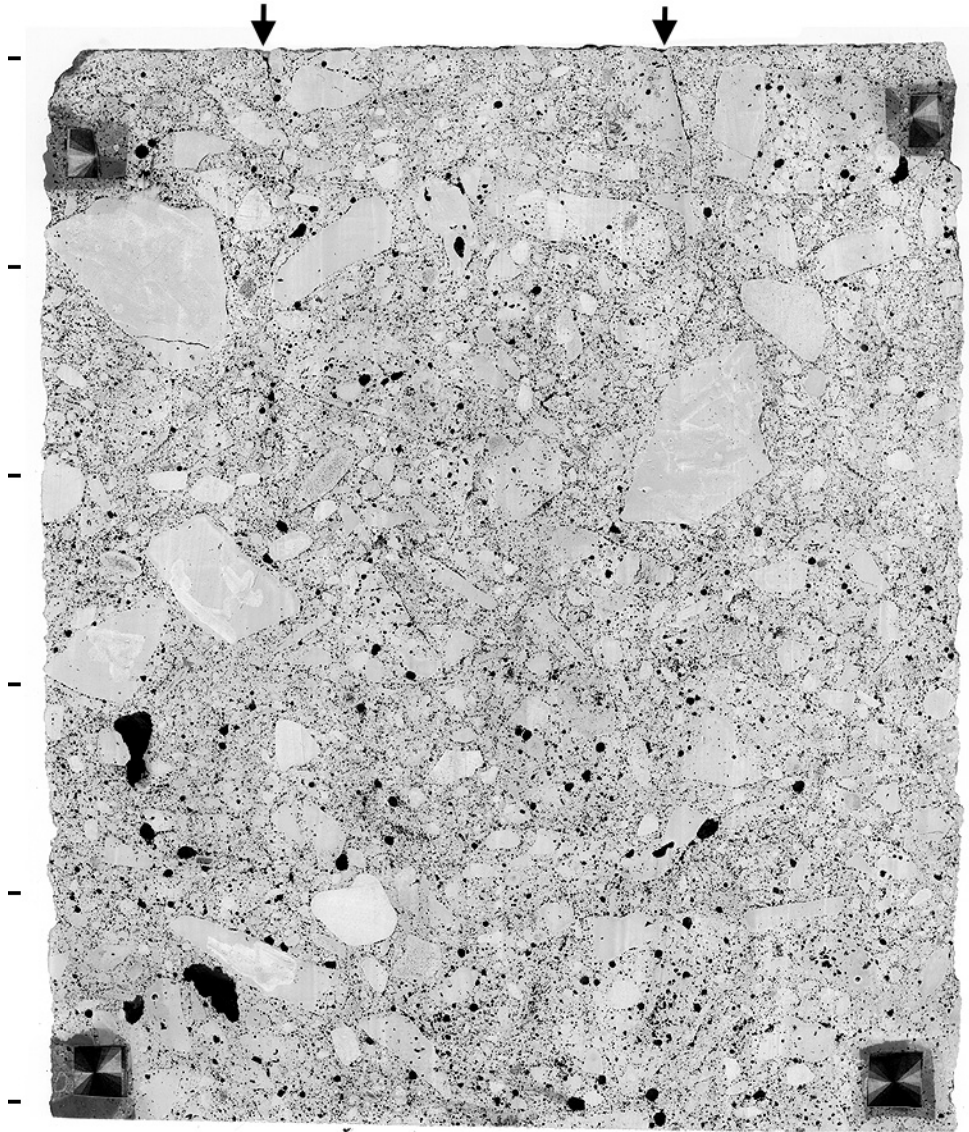


Figure A.7: Detailed scanned image from slab representing top-half of core NB-2 to illustrate cross-section of cracks observed at pavement surface, (black arrows) tic marks along left-hand side spaced at 1" intervals. Prismatic stickers at the four-corners were applied to assist with automated air void analysis.

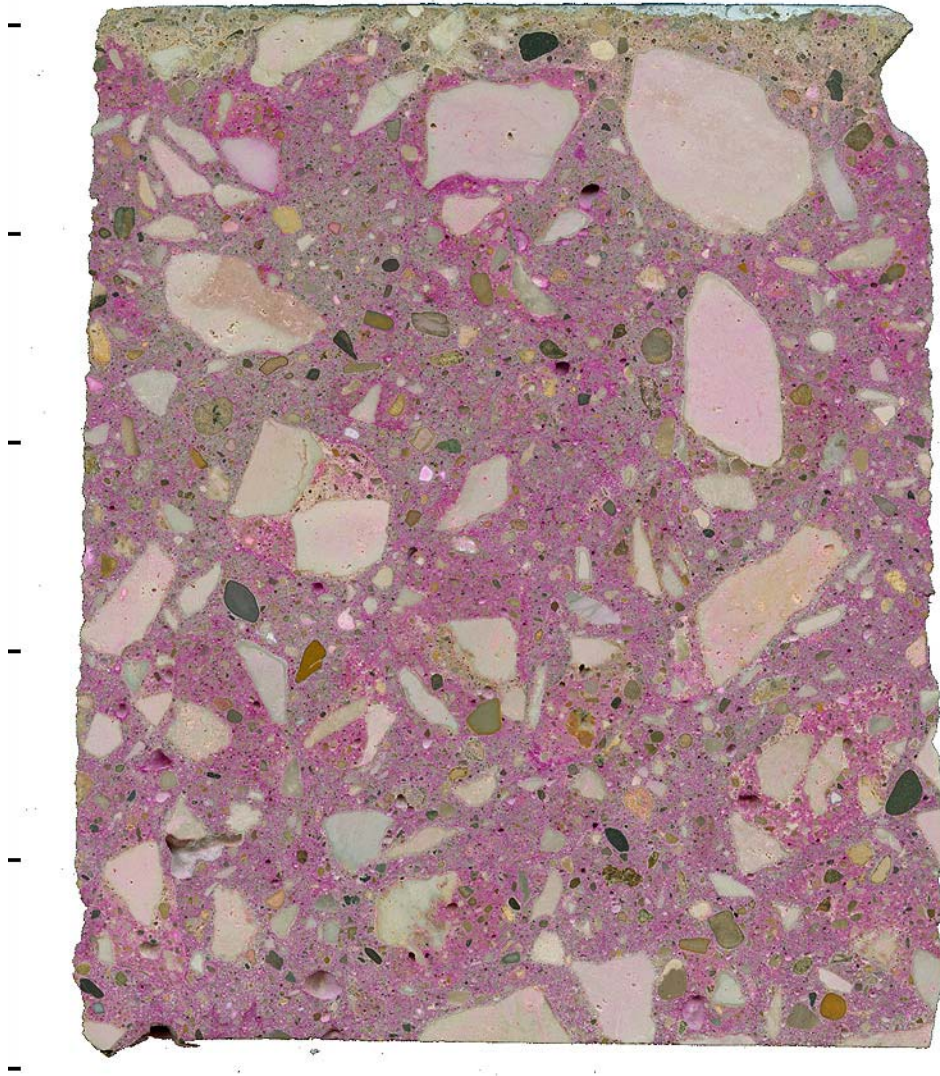


Figure A.8: Detailed scanned image from slab representing top-half of core SB-2 to illustrate depth of carbonation (approximately 1/4").



Figure A.9: Detailed scanned image from slab representing top-half of core SB-2 to illustrate extent of yellow sodium cobaltinitrite stained regions.

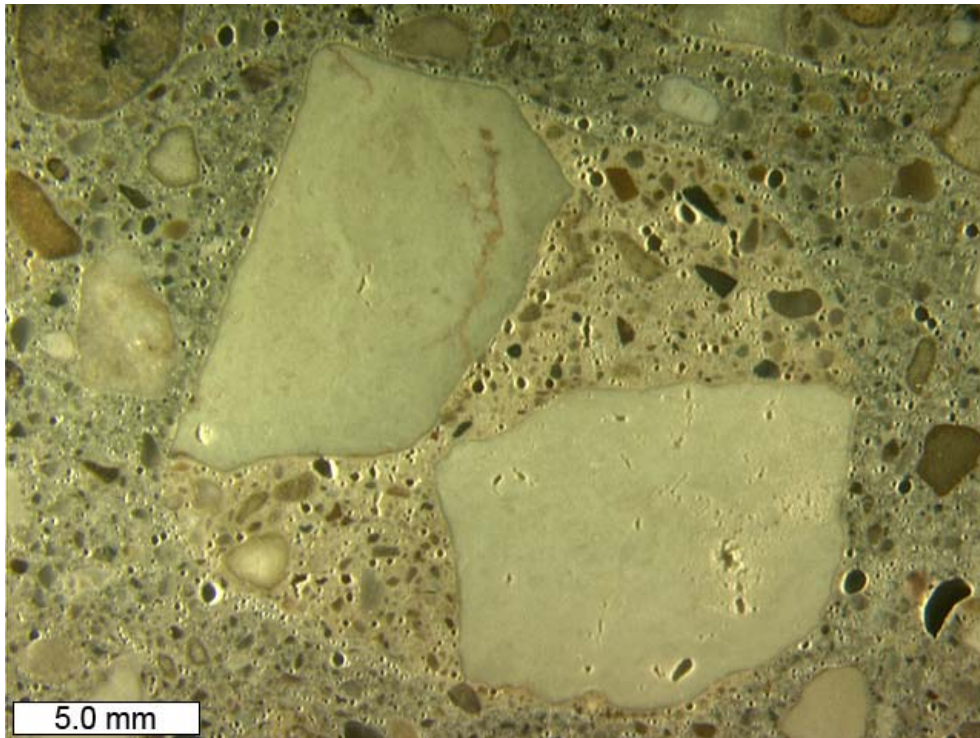


Figure A.10: Example of large recycled coarse aggregate particle in polished cross-section, core NB-2.

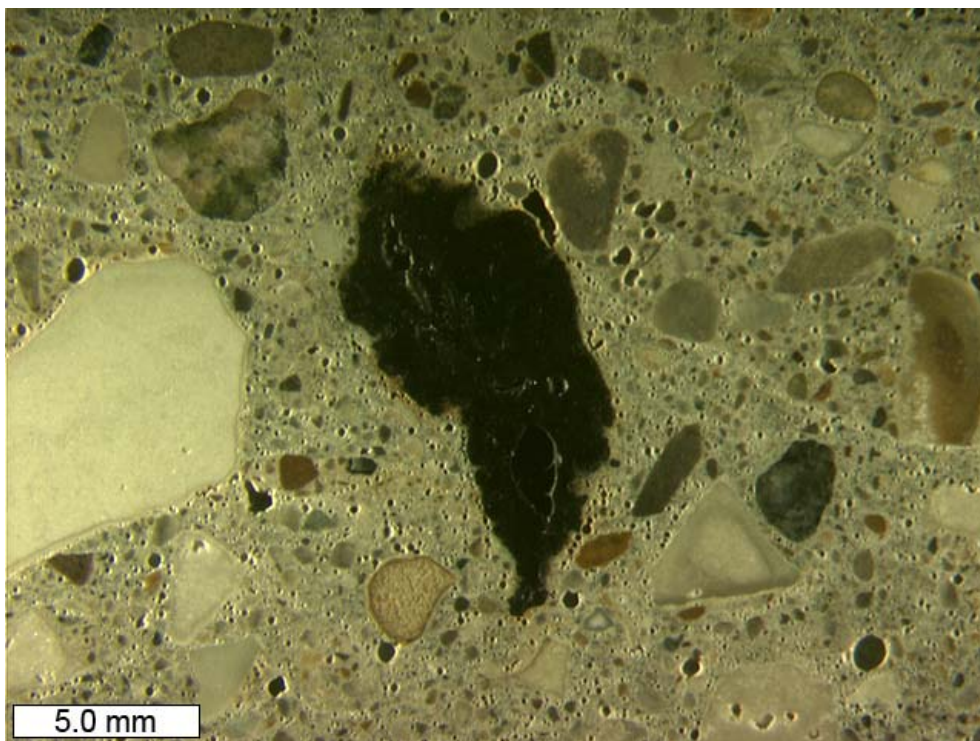


Figure A.11: Lump of asphalt observed in polished cross-section, core NB-2.

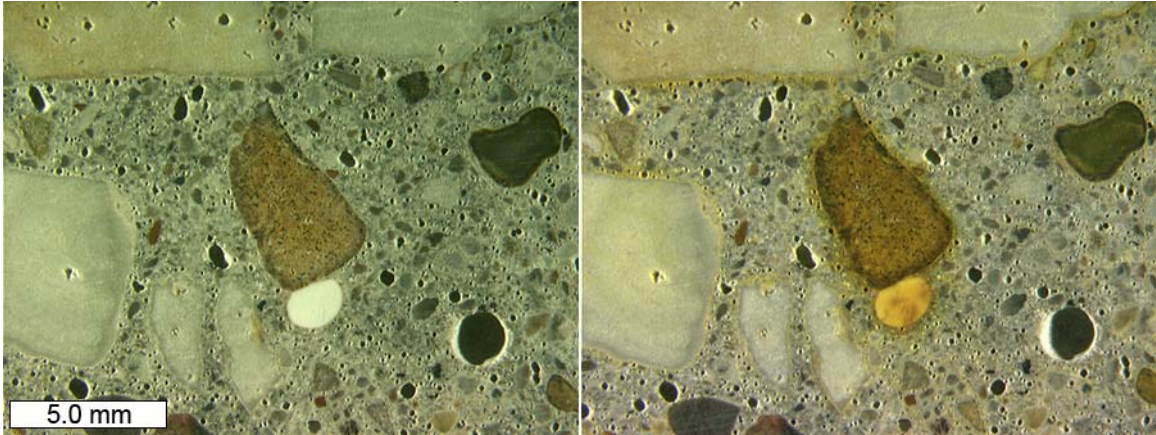


Figure A.12: Reactive fine aggregate particle with adjacent blob of alkali-silica reaction product, core NB-2, both before, (left) and after sodium cobaltinitrite stain, (right).

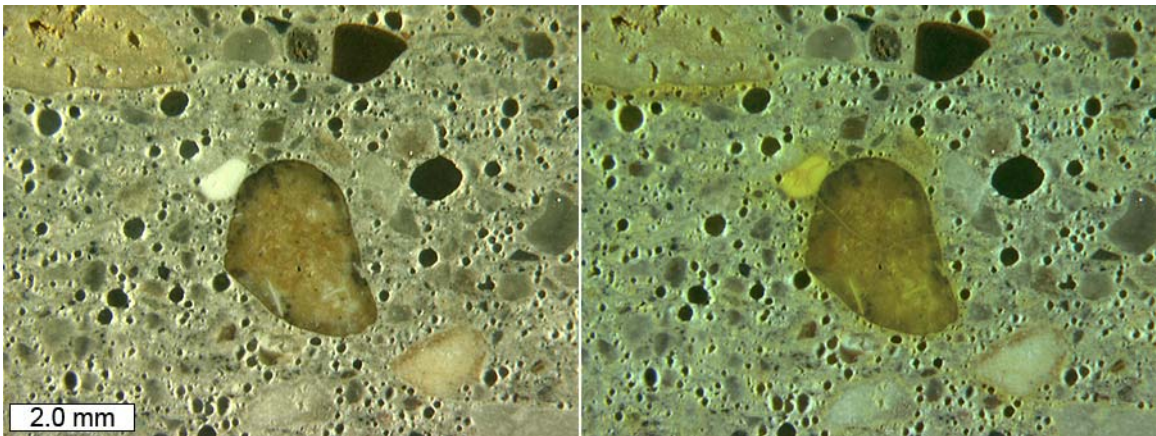


Figure A.13: Reactive fine aggregate particle with fine cracks and adjacent blob of alkali-silica reaction product, core SB-2, both before, (left) and after sodium cobaltinitrite stain, (right).

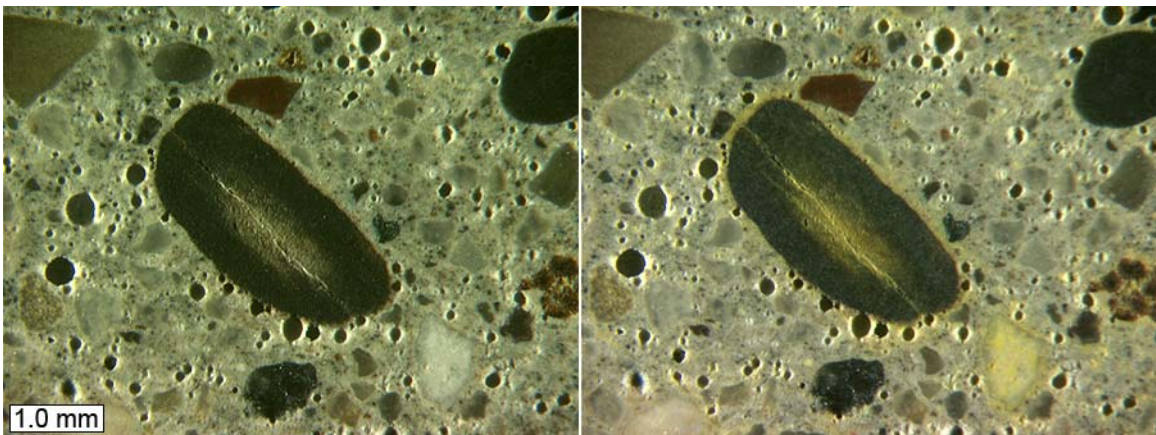


Figure A.14: Reactive fine aggregate particle with fine cracks, core SB-2, both before, (left) and after sodium cobaltinitrite stain, (right).

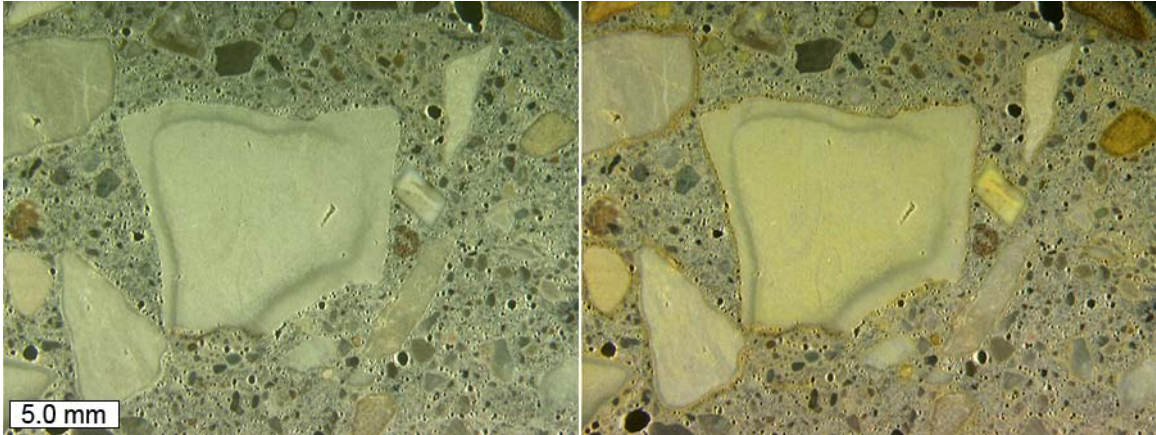


Figure A.15: Carbonate fraction of recycled coarse aggregate particles, core NB-2, both before, (left) and after sodium cobaltinitrite stain, (right).

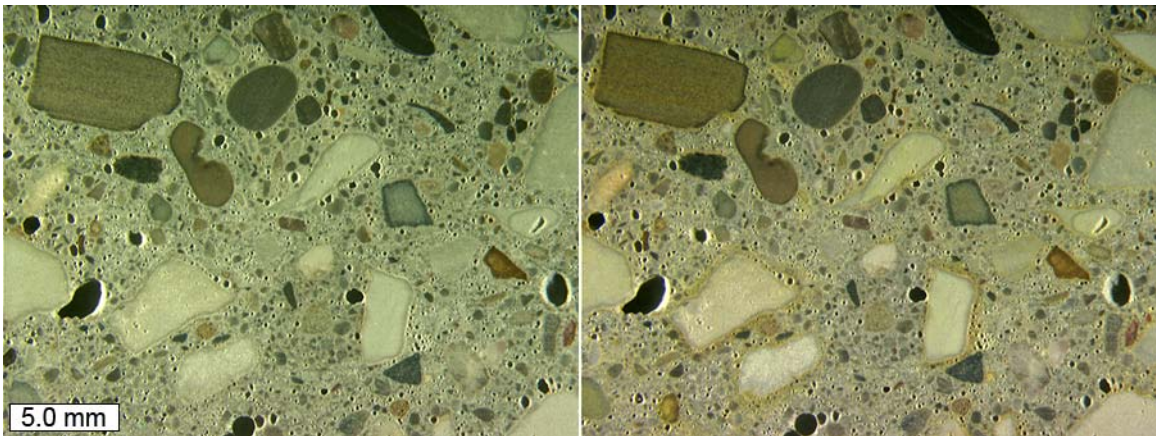


Figure A.16: Carbonate fraction of recycled coarse aggregate particles, core NB-2, both before, (left) and after sodium cobaltinitrite stain, (right).

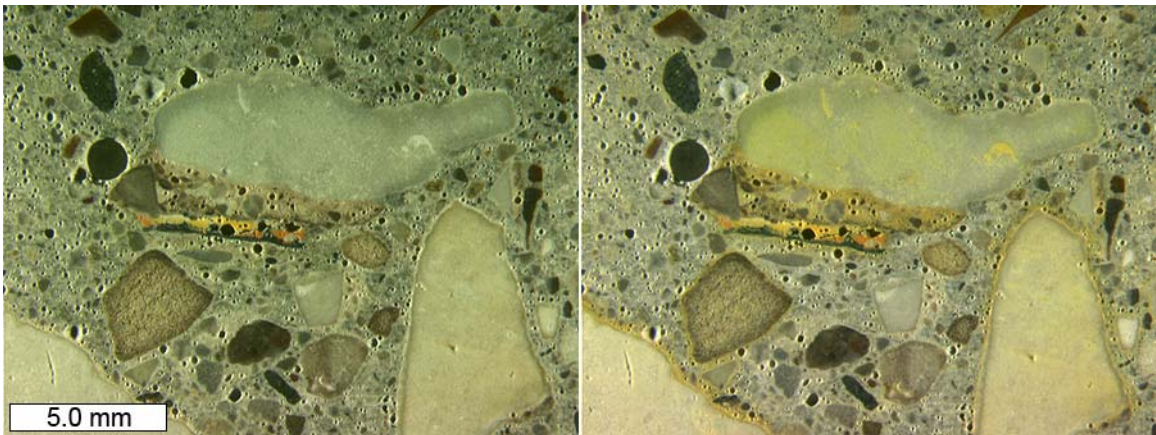


Figure A.17: Carbonate fraction of recycled coarse aggregate particles, one with adhered paint from original concrete surface, core SB-2, both before, (left) and after sodium cobaltinitrite stain, (right).

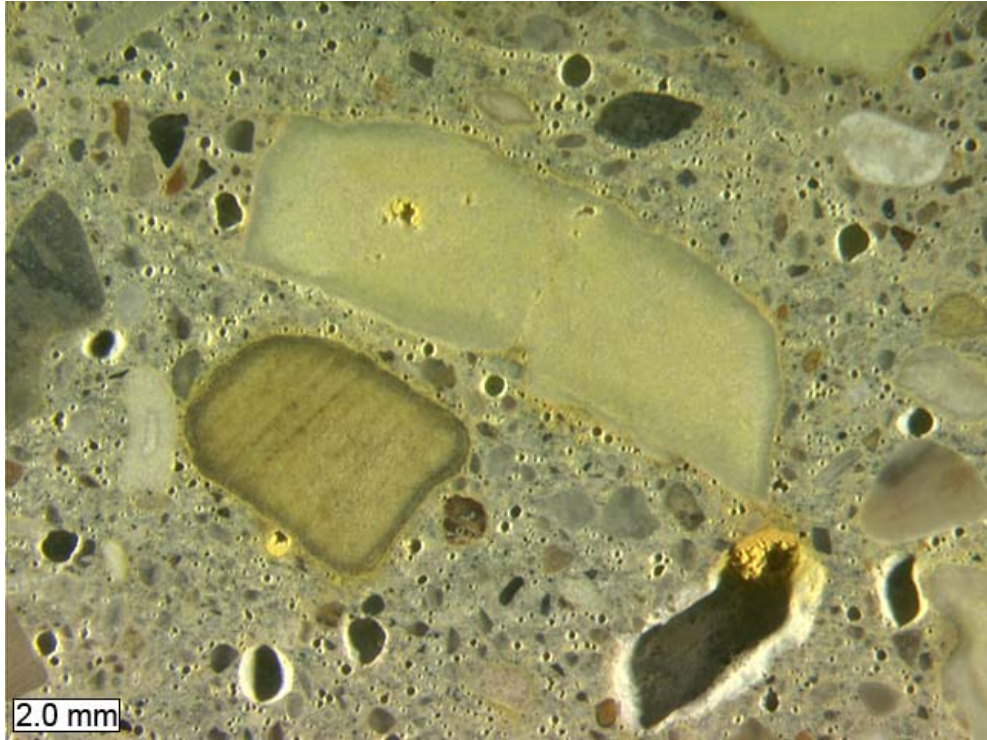
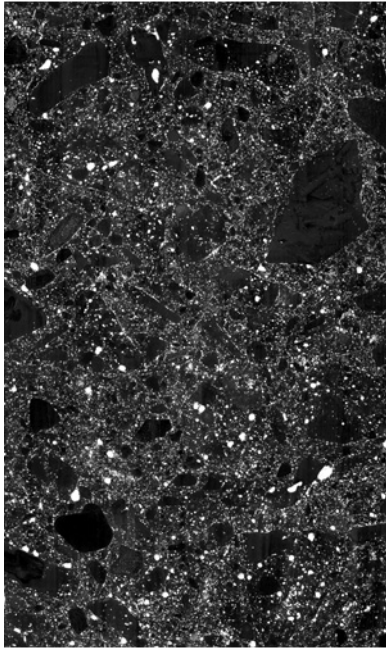


Figure A.18: Examples of alkali-silica reaction product filling voids near reactive aggregate particles, after application of sodium cobaltinitrite stain, core SB-2.

## Results of Automated Air Void Analyses

**Air Void Analysis of Hardened Concrete**  
**Calculated According to ASTM C 457**



Scanned Black and White Image

Scanned Image After Thresholding

Area Analyzed (mm x mm)

69 x 115

---

<b>Sample #:</b>	NB2_A_top_bw	<b>Date:</b>	8/21/08 10:29 AM
<b>Project ID:</b>	IDOT I57	<b>Test Lab:</b>	MTU
<b>Originator:</b>	Jeff Roesler	<b>Threshold:</b>	149
<b>Operator:</b>	Karl Peterson	<b># Iterations:</b>	3
<b>File Name:</b>	C:\Program Files\AirVoids\ScannedImages\NB2_A_top_bw.tif		

---

***MichiganTech***

## Air Void Analysis of Hardened Concrete

### Calculated According to Procedure A

#### Results

<b># of Pixels in Traverse Line:</b>	822168
<b>Resolution (microns/pixel):</b>	8
<b>Length of Traverse (mm):</b>	6577.3
<b># of Air Pixels:</b>	88165
<b># of Non-air Pixels:</b>	734003
<b># of Air Void Chord Intercepts:</b>	6195
<b>Calculated Air Content (%):</b>	10.723
<b>Paste Content (%):</b>	40.000
<b>Paste/Air Ratio:</b>	3.730
<b>Void Frequency (Voids/mm):</b>	0.942
<b>Specific Surface (mm<sup>2</sup>/mm<sup>3</sup>):</b>	35.133
<b>Powers Spacing Factor (mm):</b>	0.106

---

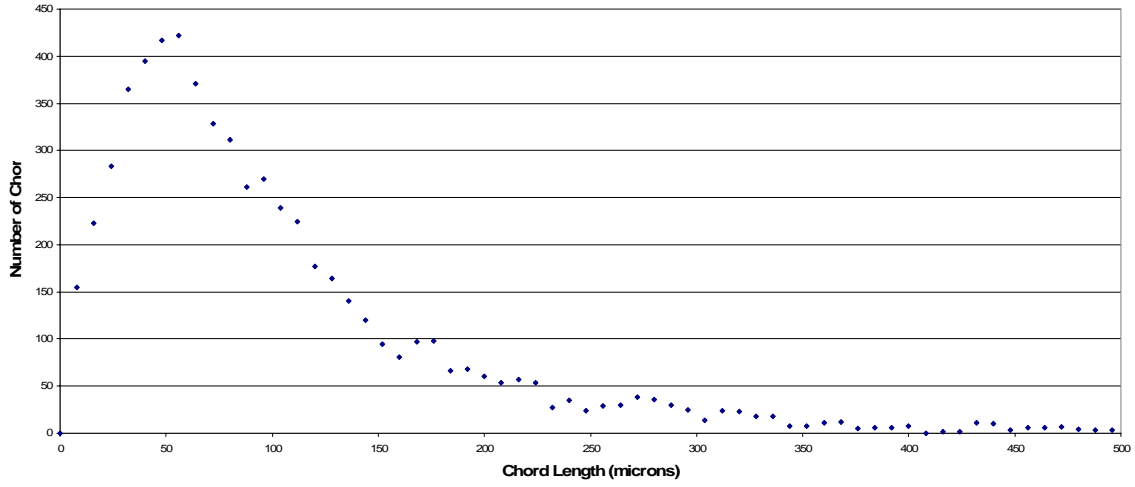
<b>Sample #:</b>	NB2_A_top_bw	<b>Date:</b>	8/21/08 10:29 AM
<b>Project ID:</b>	IDOT I57	<b>Test Lab:</b>	MTU
<b>Originator:</b>	Jeff Roesler	<b>Threshold:</b>	149
<b>Operator:</b>	Karl Peterson	<b># Iterations:</b>	3
<b>File Name:</b>	C:\Program Files\AirVoids\ScannedImages\NB2_A_top_bw.tif		

---

***MichiganTech.***

# Air Void System - Graphical Analysis

## Distribution of Air-Void Chord Lengths



Comments....

---

---

---

---

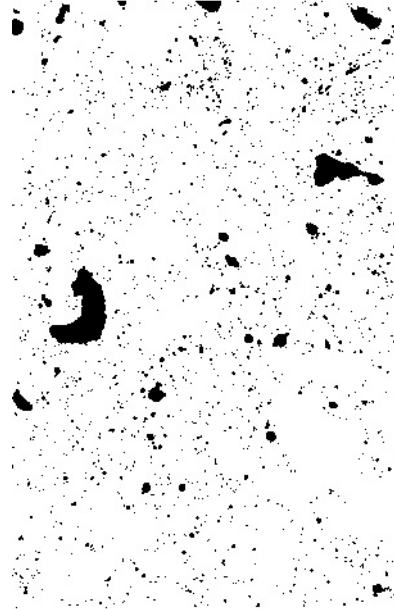
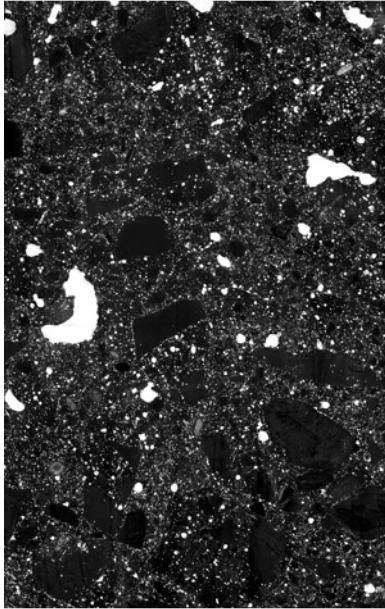
---

---

---

---

**Air Void Analysis of Hardened Concrete**  
**Calculated According to ASTM C 457**



Scanned Black and White Image

Scanned Image After Thresholding

Area Analyzed (mm x mm)

72 x 113

---

<b>Sample #:</b>	NB2_A_bot_bw	<b>Date:</b>	8/21/08 10:34 AM
<b>Project ID:</b>	IDOT I57	<b>Test Lab:</b>	MTU
<b>Originator:</b>	Jeff Roesler	<b>Threshold:</b>	149
<b>Operator:</b>	Karl Peterson	<b># Iterations:</b>	3
<b>File Name:</b>	C:\Program Files\AirVoids\ScannedImages\NB2_A_bot_bw.tif		

---

***MichiganTech***

## Air Void Analysis of Hardened Concrete Calculated According to Procedure A

### Results

<b># of Pixels in Traverse Line:</b>	807006
<b>Resolution (microns/pixel):</b>	8
<b>Length of Traverse (mm):</b>	6456.0
<b># of Air Pixels:</b>	88086
<b># of Non-air Pixels:</b>	718920
<b># of Air Void Chord Intercepts:</b>	4503
<b>Calculated Air Content (%):</b>	10.915
<b>Paste Content (%):</b>	40.000
<b>Paste/Air Ratio:</b>	3.665
<b>Void Frequency (Voids/mm):</b>	0.697
<b>Specific Surface (mm<sup>2</sup>/mm<sup>3</sup>):</b>	25.560
<b>Powers Spacing Factor (mm):</b>	0.143

---

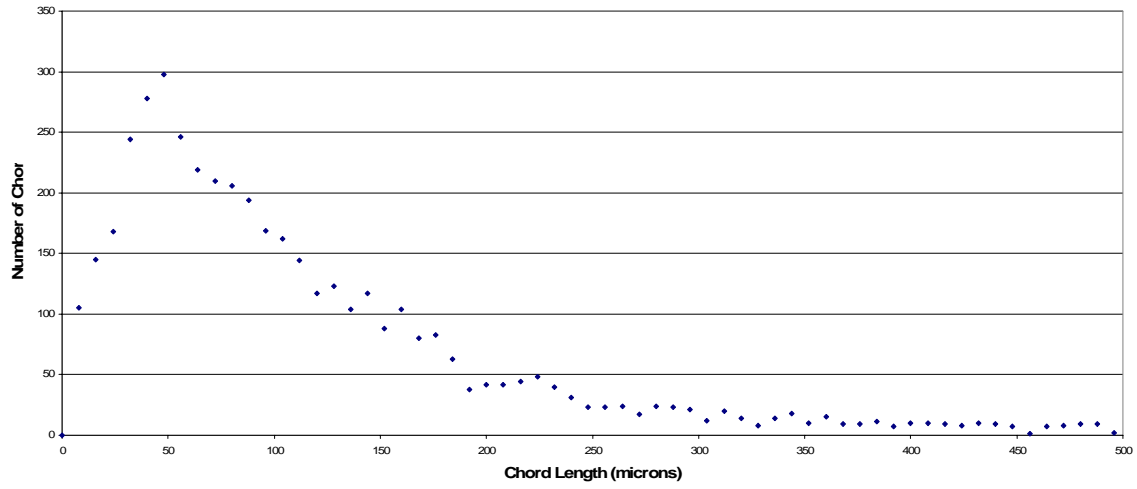
<b>Sample #:</b>	NB2_A_bot_bw	<b>Date:</b>	8/21/08 10:34 AM
<b>Project ID:</b>	IDOT I57	<b>Test Lab:</b>	MTU
<b>Originator:</b>	Jeff Roesler	<b>Threshold:</b>	149
<b>Operator:</b>	Karl Peterson	<b># Iterations:</b>	3
<b>File Name:</b>	C:\Program Files\AirVoids\ScannedImages\NB2_A_bot_bw.tif		

---

***MichiganTech.***

# Air Void System - Graphical Analysis

## Distribution of Air-Void Chord Lengths



Comments....

---

---

---

---

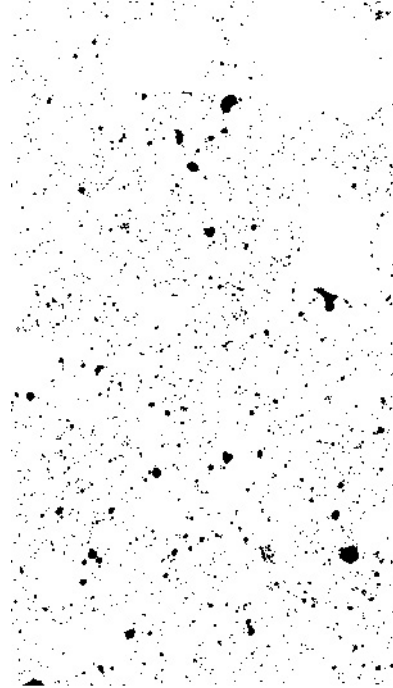
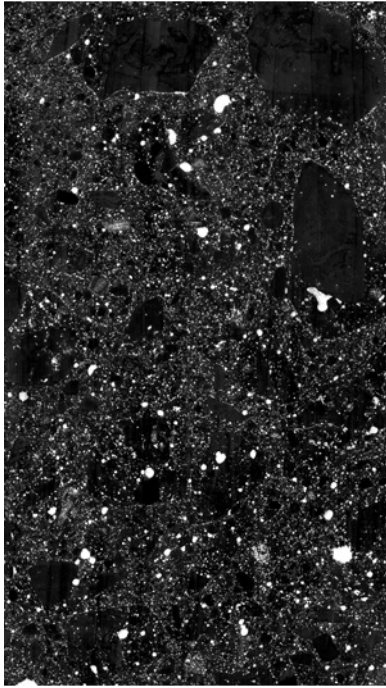
---

---

---

---

**Air Void Analysis of Hardened Concrete**  
**Calculated According to ASTM C 457**



Scanned Black and White Image

Scanned Image After Thresholding

Area Analyzed (mm x mm)

64 x 113

---

<b>Sample #:</b>	SB2_A_top_bw	<b>Date:</b>	8/21/08 10:38 AM
<b>Project ID:</b>	IDOT I57	<b>Test Lab:</b>	MTU
<b>Originator:</b>	Jeff Roesler	<b>Threshold:</b>	149
<b>Operator:</b>	Karl Peterson	<b># Iterations:</b>	3
<b>File Name:</b>	C:\Program Files\AirVoids\ScannedImages\SB2_A_top_bw.tif		

---

***MichiganTech.***

## Air Void Analysis of Hardened Concrete Calculated According to Procedure A

### Results

<b># of Pixels in Traverse Line:</b>	807861
<b>Resolution (microns/pixel):</b>	8
<b>Length of Traverse (mm):</b>	6462.9
<b># of Air Pixels:</b>	68295
<b># of Non-air Pixels:</b>	739566
<b># of Air Void Chord Intercepts:</b>	4437
<b>Calculated Air Content (%):</b>	8.454
<b>Paste Content (%):</b>	40.000
<b>Paste/Air Ratio:</b>	4.732
<b>Void Frequency (Voids/mm):</b>	0.687
<b>Specific Surface (mm<sup>2</sup>/mm<sup>3</sup>):</b>	32.484
<b>Powers Spacing Factor (mm):</b>	0.139

---

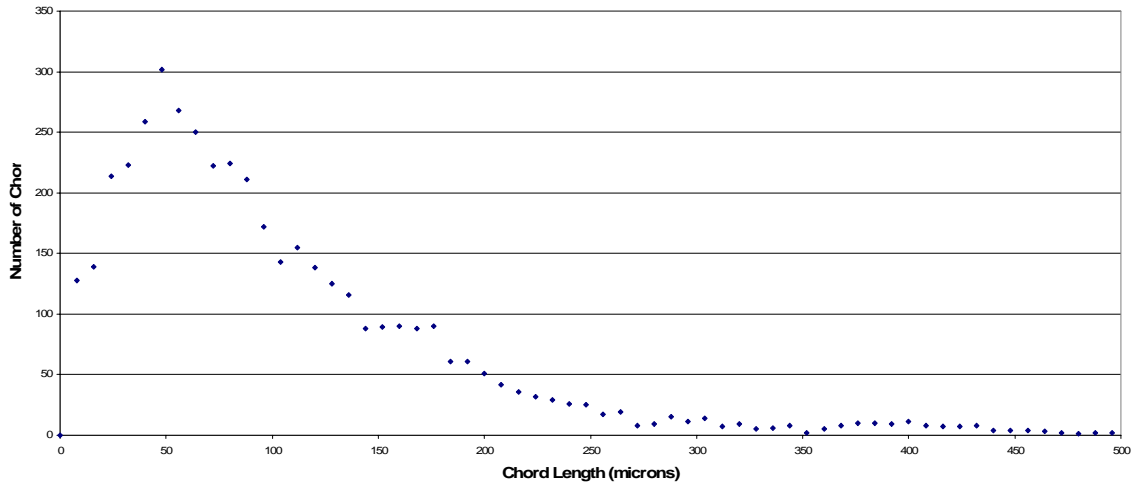
<b>Sample #:</b>	SB2_A_top_bw	<b>Date:</b>	8/21/08 10:38 AM
<b>Project ID:</b>	IDOT I57	<b>Test Lab:</b>	MTU
<b>Originator:</b>	Jeff Roesler	<b>Threshold:</b>	149
<b>Operator:</b>	Karl Peterson	<b># Iterations:</b>	3
<b>File Name:</b>	C:\Program Files\AirVoids\ScannedImages\SB2_A_top_bw.tif		

---

***MichiganTech.***

# Air Void System - Graphical Analysis

## Distribution of Air-Void Chord Lengths



Comments....

---

---

---

---

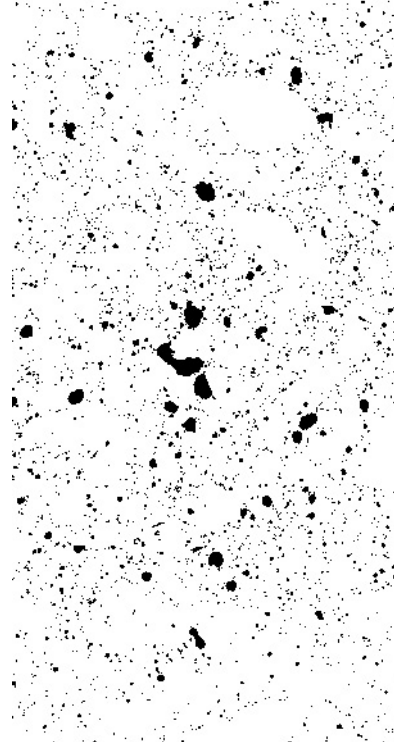
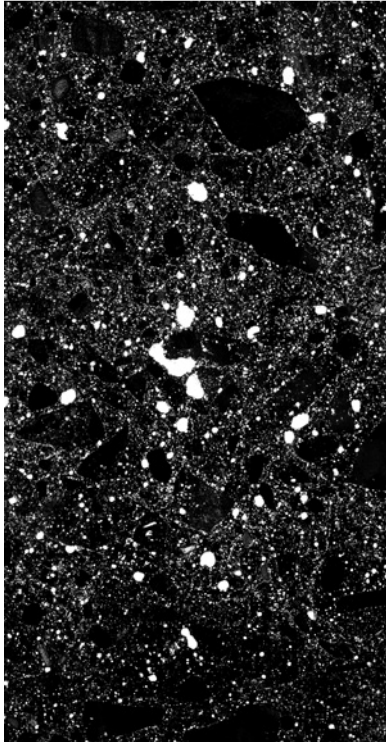
---

---

---

---

**Air Void Analysis of Hardened Concrete**  
**Calculated According to ASTM C 457**



Scanned Black and White Image

Scanned Image After Thresholding

Area Analyzed (mm x mm)

64 x 124

---

<b>Sample #:</b>	SB2_A_bot_bw	<b>Date:</b>	8/21/08 10:43 AM
<b>Project ID:</b>	IDOT I57	<b>Test Lab:</b>	MTU
<b>Originator:</b>	Jeff Roesler	<b>Threshold:</b>	149
<b>Operator:</b>	Karl Peterson	<b># Iterations:</b>	3
<b>File Name:</b>	C:\Program Files\AirVoids\ScannedImages\SB2_A_bot_bw.tif		

---

***MichiganTech.***

## Air Void Analysis of Hardened Concrete

### Calculated According to Procedure A

#### Results

<b># of Pixels in Traverse Line:</b>	883956
<b>Resolution (microns/pixel):</b>	8
<b>Length of Traverse (mm):</b>	7071.6
<b># of Air Pixels:</b>	103743
<b># of Non-air Pixels:</b>	780213
<b># of Air Void Chord Intercepts:</b>	5737
<b>Calculated Air Content (%):</b>	11.736
<b>Paste Content (%):</b>	40.000
<b>Paste/Air Ratio:</b>	3.408
<b>Void Frequency (Voids/mm):</b>	0.811
<b>Specific Surface (mm<sup>2</sup>/mm<sup>3</sup>):</b>	27.650
<b>Powers Spacing Factor (mm):</b>	0.123

---

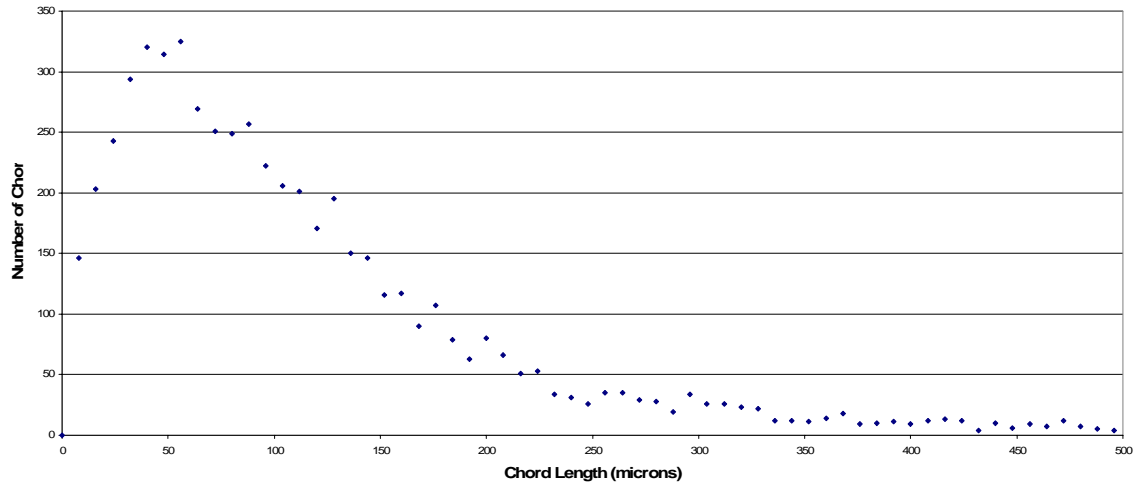
<b>Sample #:</b>	SB2_A_bot_bw	<b>Date:</b>	8/21/08 10:43 AM
<b>Project ID:</b>	IDOT I57	<b>Test Lab:</b>	MTU
<b>Originator:</b>	Jeff Roesler	<b>Threshold:</b>	149
<b>Operator:</b>	Karl Peterson	<b># Iterations:</b>	3
<b>File Name:</b>	C:\Program Files\AirVoids\ScannedImages\SB2_A_bot_bw.tif		

---

***MichiganTech.***

# Air Void System - Graphical Analysis

## Distribution of Air-Void Chord Lengths



Comments....

---

---

---

---

---

---

---

---

